

Amine-Mediated Electrochemical Reduction of CO₂ in a Nonaqueous, Li-CO₂ Battery

by

Aliza Khurram

Bachelor of Science, Physics and Mathematics

Bates College, 2015

SUBMITTED TO THE DEPARTMENT OF MECHANICAL ENGINEERING IN
PARTIAL FULFILLMENT OF THE REQUIREMENTS FOR THE DEGREE OF

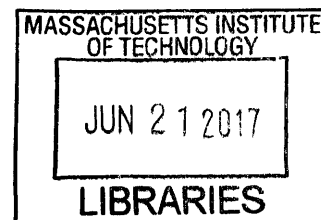
MASTER OF SCIENCE IN MECHANICAL ENGINEERING

at the

MASSACHUSETTS INSTITUTE OF TECHNOLOGY

June 2017

© 2017 Massachusetts Institute of Technology
All rights reserved.



Signature redacted

Signature of Author: _____

A handwritten signature in black ink, appearing to be "Aliza Khurram".

Department of Mechanical Engineering
May 15, 2017

Signature redacted

Certified By: _____

Betar M. Gallant
Assistant Professor of Mechanical Engineering
Thesis Supervisor

Signature redacted

Accepted By: _____

Rohan Abeyratne
Professor of Mechanical Engineering
Chairman, Department Graduate Committee

Amine-Mediated Electrochemical Reduction of CO₂ in a Nonaqueous, Li-CO₂ Battery

By
Aliza Khurram

Submitted to the Department of Mechanical Engineering
on May 15, 2017
in Partial Fulfillment of the Requirements for the Degree of
Master of Science in Mechanical Engineering

ABSTRACT

The development of effective CO₂ capture and conversion methods is not only crucial for mitigating rising global atmospheric CO₂ concentrations but also for exploiting atmospheric carbon dioxide as a potential source of C₁ feedstock for the industrial synthesis of fuels and chemicals. Herein, we report a combined chemical-electrochemical device for post-combustion capture and subsequent conversion of CO₂ into a benign, solid alkali metal-containing phase (lithium carbonate, Li₂CO₃). The capture is accomplished in a non-aqueous battery electrolyte containing a molecular CO₂ sorbent, and the conversion is initiated at an electrode surface, which advantageously combines two conventionally separate approaches to CO₂ mitigation. In particular, the proposed system utilizes an amine, namely 2-ethoxyethylamine (EEA) in an organic electrolyte (dimethyl sulfoxide) to activate the CO₂ molecule via chemisorption prior to electrochemical reduction at a simple carbon electrode in a Li-CO₂ battery configuration. We show that by decoupling the first electron transfer step from the structural rearrangement of the CO₂ molecule, we are able to electrochemically reduce CO₂ kinetically accessible.

In order to demonstrate that bending the CO₂ molecule prior to delivering it to an electrode surface for reduction facilitates the rate limiting step in classical electrochemical reduction, we investigated the energetics of chemically complexed CO₂ reduction via galvanostatic discharge testing of Li-CO₂ cells. Our results indicate that the electrochemical reduction of complexed amines containing the bent CO₂ molecules proceed at significantly higher discharge potentials (~3 V vs. Li) compared to the gaseous, dissolved (uncomplexed) CO₂, the gaseous, physically absorbed CO₂, and yield high discharge capacities (> 1000 mAh/g_C), thus functioning effectively as a primary battery. To elucidate the reaction mechanism, we employed a series of solid-phase product characterization techniques. Our

results revealed that the proposed system converts bound CO₂ to primarily solid-phase amorphous lithium carbonate, which has the potential to eliminate the energetic and logistical costs associated with long-term underground storage of compressed CO₂ in conventional carbon capture technologies. Additionally, through liquid phase analyses, we present evidence for selective cleavage of the bond -N-C- (i.e. the bond formed between the amine and CO₂ when amine binds the CO₂ molecule) upon electrochemical reduction of loaded amine species. Furthermore, an analysis of the system's performance under varying conditions such as applied current density and amine concentration is presented. The likely full cell reaction, the possibility of formation of any secondary products and final state of the amine is also discussed.

ACKNOWLEDGEMENTS

I owe a debt of gratitude to Prof. Betar Gallant without whose unwavering guidance and support, none of this would have been possible. Her intellectual and personal generosity continually inspire me to be both a better researcher and a better person. Thank you for being such a role model! Your words of encouragement were central to my decision to come to MIT and have continued to sustain me through my toughest times here. Working with you and learning from you has been an absolute honor.

To my friends, thank you for always looking out for me. Thank you to Ness who has truly redefined what it means to have a best friend. Grad school life as I know it would not have been possible without you taking the burden of cooking, laundry and all other life-sustaining chores from me. Thank you to Mahnum, who has had my back for the last ten years and whose knowledge of chemistry, English grammar and patience have been tested to their limit during the writing of this thesis. A special thanks to Roch, for always making me laugh. And thank you to my lab mates and all the wonderful friends I have made at MIT and beyond who inspire me not only for their intellectual prowess but also their humanity.

And finally, thank you to my parents and siblings whose unconditional love and support have kept me afloat all these years. Your faith, your wisdom and your endless dedication to helping me be the best version of myself has enabled everything. Thank you for believing in me. I hope I can make you proud.

Table of Contents

Abstract	ii
Acknowledgements	iv
1. INTRODUCTION	1
1.1 Carbon Dioxide: Primary Sources and Emissions	1
1.2 CO ₂ Electronic Structure as a Predictor of Reactivity	4
1.3 Current CO ₂ Mitigation Approaches	5
1.3.1 Carbon Capture and Sequestration (CCS) Technologies.....	6
1.3.2 Electrochemical CO ₂ Reduction	17
1.4 Combined Chemical-Electrochemical CO ₂ Capture and Conversion.....	24
2. EXPERIMENTAL DETAILS	26
3. RESULTS	34
3.1 Electrolyte Design.....	34
3.1.1 Products of Amine-CO ₂ Complexation in Non-Aqueous Electrolytes	34
3.2 Electrochemical Testing of Li-CO ₂ Cells with Amine Additives	40
3.2.1 Reduction of Complexed Amine Species in a non-aqueous Li-CO ₂ cell	40
3.2.2 Effect of Amine Concentration on Discharge Capacity	42
3.3 Solid-Phase Discharge Product Characterization	44
3.4 Detection of Potential Secondary Products.....	49
3.5 Fate of the Amine upon Electrochemical Reduction of Complexed Amine Species ..	51
3.6 Cyclic Voltammetry Studies on the Reduction of Loaded Amine Species	54
3.7 Experimental Determination of the Maximum Achievable Potential.....	56
4. ADVANTAGES OF AMINE-MEDIATED NON-AQUEOUS CO₂ REDUCTION ..	58
5. CONCLUSION AND FUTURE WORKS	62
6. REFERENCES	67

List of Figures

Figure 1-1: Evolution of atmospheric CO ₂ concentration and global annual average temperature with time. Figure by NOAA/NCDC: https://www.ncdc.noaa.gov/monitoring-references/faq/indicators.php	1
Figure 1-2: The three resonance structures of the linear CO ₂ molecule.	5
Figure 1-3: Mechanism of carbamate formation from the chemical absorption of 1 mole of CO ₂ by 2 moles of a primary amine, MEA via a zwitterion intermediate.	8
Figure 1-4: Formation of bicarbonate upon reaction of one mole of tertiary amine dimethylaminoethanol (DMAE) with one mole of CO ₂ in water.	9
Figure 1-5: Schematic representation of a typical thermal amine scrubbing process. ¹⁴	10
Figure 1-6: Reaction between an imidazolium-based ionic liquid and CO ₂ to form carbamate.	13
Figure 1-7: The EMAR cycle. ¹⁴	15
Figure 1-8: Schematic comparing the proposed approach (b) with the classically employed approach (a) for CO ₂ reduction.	25
Figure 2-1: Schematic representation of an Li-CO ₂ Swagelok cell.	27
Figure 2-2: Schematic representation of a three-electrode electrolysis type cell.	30
Figure 3-1: Hydrogen-bonded interactions between -CO ₂ H group of the carbamic acid and S=O group of DMSO. ¹²	37
Figure 3-2: ¹ H NMR spectra of 50 mM lean EEA (top) and loaded EEA (bottom) in DMSO-d ₆	37
Figure 3-3: Mechanism of carbamate and carbamic acid formation from the chemical absorption of CO ₂ by the primary amine EEA via a zwitterion intermediate in DMSO-d ₆	38
Figure 3-4: Reaction between ammonium carbamate and lithium perchlorate to form ammonium perchlorate and lithium carbamate.	39
Figure 3-5: Photographs showing 0.5 mL of (a) pure DMSO with 2 M CO ₂ bound EEA and (b) 2 M LiClO ₄ in DMSO with 2 M CO ₂ -bound EEA.	39
Figure 3-6: Galvanostatic discharge profiles at varying current densities. The electrolyte used was 0.1 M EEA in 0.3M LiClO ₄ /DMSO.	41

Figure 3-7: Galvanostatic discharge under a pure CO ₂ headspace without the addition of amine. The electrolyte used was 0.3 M LiClO ₄ /DMSO.	41
Figure 3-8: Galvanostatic discharge under a pure CO ₂ headspace without the addition of amine. The electrolyte used was 0.3 M LiClO ₄ /DMSO.	42
Figure 3-9: Galvanostatic discharge at 30 mA/g at varying amine concentrations. The electrolyte used was 0.3 M LiClO ₄ in DMSO.....	43
Figure 3-10: Plot of discharge capacity vs. amine concentration indicating an optimal amine concentration.....	44
Figure 3-11: Infrared spectra of (a) carbon cathode after a galvanostatic discharge at 30 mA/g _{carbon} with 0.1 M EEA; (b) carbon cathode after a galvanostatic discharge at 30 mA/g _{carbon} with no amine; (c) a pristine cathode; and (d) the electrode from (a) after treatment with 2 M H ₃ PO ₄	45
Figure 3-12: X-Ray diffraction scans of a pristine and a galvanostatically discharged Toray paper electrode. The applied current density was 30 mA/g and the electrolyte used was 0.1 M EEA in 0.3 M LiClO ₄ in DMSO. The XRD spectrum of crystalline lithium carbonate is provided as a reference.	46
Figure 3-13: SEM images of (a) pristine cathode and (b) discharged cathode (Vulcan Carbon) at 30 mA/g. The electrolyte used was 100 mM EEA in 0.3 M LiClO ₄ in DMSO.....	47
Figure 3-14: SEM images of (a) pristine cathode and (b) discharged cathode (GDL) at 30 mA/g. The electrolyte used was 100 mM EEA in 0.3 M LiClO ₄ in DMSO. The top and bottom row images have a corresponding magnification of 10Kx and 20Kx respectively.	48
Figure 3-15: Infrared spectra of (a) GDL electrode after a galvanostatic discharge at 30 mA/g _{carbon} with 0.1 M EEA and (b) pristine GDL electrode.	49
Figure 3-16: Galvanostatic discharge on GDL electrodes at varying current densities (a) and the corresponding ⁷ Li NMR spectra obtained for Li ₂ CO ₃ quantification. The electrolyte used was 0.1 M EEA in 0.3 M LiClO ₄ in DMSO.	50
Figure 3-17: ¹³ C NMR spectrum of 50 mM EEA in 0.3M LiClO ₄ in DMSO prior to reduction (a), post electrochemical reduction (b), and CO ₂ purge after reduction (c).....	53
Figure 3-18: ¹ H NMR spectrum of 50 mM EEA in 0.3M LiClO ₄ in DMSO-d ₆ (not deuterated) following electrochemical reduction.....	54

Figure 3-19: Reduction of loaded amine species on glassy carbon at 0.2 mV/s. The electrolyte used was 50 mM EEA in 0.3 M LiClO₄ in DMSO. 55

Figure 3-20: Reduction of loaded amine species on glassy carbon at 0.2 mV/s at varying rotation rates. The electrolyte used was 50 mM EEA in 0.3 M LiClO₄ in DMSO. 56

Figure 3-21: Potentiodynamic cycling with galvanostatic acceleration (PCGA) discharge of a Vulcan carbon electrode from open circuit (~3.05 V vs. Li). The potential step amplitude was 5 mV and the current cutoff per step was 0.5 mA/g_c. 57

Figure 5-1: Schematic of an amine-mediated electrochemical CO₂ reduction process in non-aqueous media. 65

List of Tables

Table 1-1: Primary anthropogenic CO ₂ sources and emissions.	2
Table 1-2: Examples of primary, secondary and tertiary amines. The amine structure and pKa value corresponding to each type is provided.	7
Table 1-3: Common cations and anions employed in ionic liquids used for CO ₂ capture. ²⁴ .	12
Table 1-4: Possible CO ₂ reduction reactions in aqueous media. The provided potentials have all been measured on the copper electrode. ³⁴ The oxidation state of carbon is denoted by O.S. in the above table.	18
Table 1-5: Properties of electrode materials that have been previously investigated in literature for their catalytic behavior in aqueous CO ₂ reduction. ⁴²	19
Table 1-6: CO ₂ solubility in select organic solvents at 298 K and 1 atm.	22
Table 1-7: Possible CO ₂ reduction reactions in non-aqueous, lithium based systems. The thermodynamic parameters associated with each reaction are provided.	22
Table 1-8: Mass densities of potential products that can be formed from the electrochemical reduction of CO ₂ in either aqueous or non-aqueous media.	23
Table 3-1: Photographs of electrolyte or solvent samples containing complexed amine species indicating the feasibility of DMSO for use in this system.	35
Table 3-2: Lithium carbonate and carbon monoxide quantification results obtained for the cells shown in Fig. 3-14 (a).	50

1 INTRODUCTION

1.1 Carbon Dioxide: Primary Sources and Emissions

Carbon dioxide (CO₂) is one of the most potent greenhouse gases, accounting for close to 80.9% of anthropogenic greenhouse gas (GHG) emissions in the United States in 2014.¹ Atmospheric CO₂ concentrations have increased by almost 43% from 280 ppmv (parts per million by volume) in pre-industrial times to 401 ppmv in 2015.¹ High levels of carbon dioxide in the atmosphere can pose serious environmental harm due to the predicted link between atmospheric CO₂ levels and global warming (**Figure 1-1**). In accordance with the steadily increasing CO₂ levels, the average rate of global temperature change has risen from 0.06°C per decade in 1880 to 0.16°C per decade in 1970, a nearly three-fold increase.²

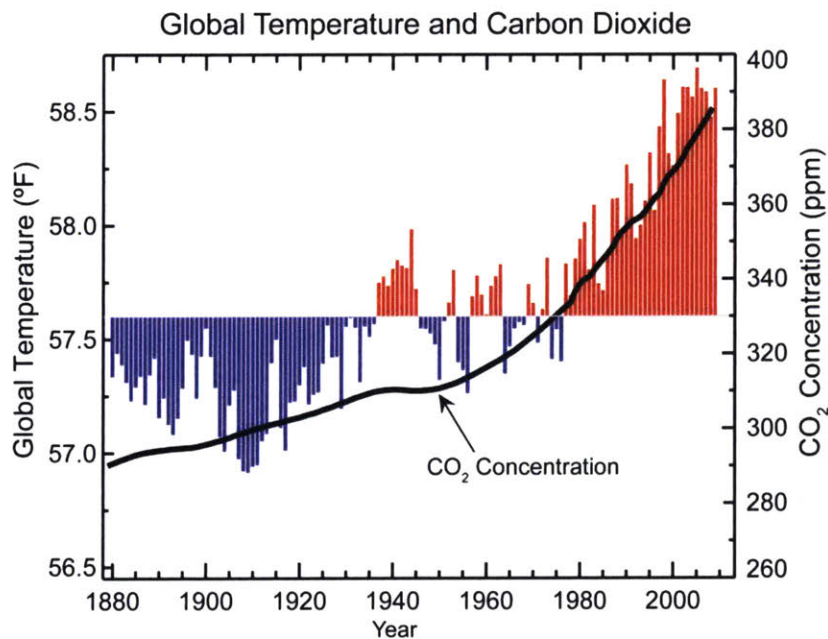


Figure 1-1: Evolution of atmospheric CO₂ concentration and global annual average temperature with time. Figure by NOAA/NCDC: <https://www.ncdc.noaa.gov/monitoring-references/faq/indicators.php>

In order to reduce the risk and impacts of climate change, both federal and international efforts are calling for increased mitigation of GHGs, and countries around the world are reaching consensus to regulate CO₂ emissions. Internationally, 141 nations have ratified the Paris Agreement, established within the United Nations Framework Convention on Climate Change (UNFCCC), which aims to limit the global temperature rise to less than 2°C this century.³ In the U.S., the Environmental Protection Agency (EPA) established the New Source Performance Standards (NSPS) under the Clean Air Act in 2016 to restrict CO₂ emissions generated from coal- and natural gas-fired power plants to 1400 lbs CO₂/MWh and 1000 lbs CO₂/MWh respectively.⁴ In light of such rigidly enforced emission standards worldwide, the need for the development of effective CO₂ mitigation systems that can curb emissions and meet stringent regulations has become increasingly imminent.

Primary Sources of CO₂	Emissions (%)
Fossil Fuel Combustion	93.7
• <i>Electricity Generation</i>	93.7
• <i>Transportation</i>	36.7
Iron, Steel and Coke Production	1.0
Natural Gas	0.8
Cement Production	0.7
Petrochemical Production	0.5

Table 1-1: Primary anthropogenic CO₂ sources and emissions.

Table 1-1 lists some key sources of anthropogenic CO₂ emissions in the U.S. in 2014. Fossil fuel combustion accounted for 93.7% of anthropogenic emissions, of which the energy and transportation sectors were key emitters. Electricity generation alone was responsible for emitting 2039.3 MMT of carbon dioxide.¹ Flue gas streams emitted from electricity generating plants, particularly those relying on coal combustion, typically contain about 11% CO₂ by volume.⁵ The substantial amount of CO₂ emissions from coal- and gas-fired power plants

highlights the central role of post-combustion carbon capture for reducing anthropogenic CO₂ emissions.

In addition to fossil fuel combustion, the cement industry is one the world's largest industrial sources of carbon dioxide emissions, releasing close to 40 MMT of CO₂ in the United States alone.¹ Cement production releases large quantities of carbon dioxide into the atmosphere as a result of both the high energy consumption of the cement making process and the chemical process itself.¹ Flue gas released from cement plants contains significantly higher CO₂ concentrations (25 % by vol)⁶ as compared to flue gas released from coal-fired power plants (11 % by vol).

Mitigation of CO₂ emissions can be achieved primarily by (i) reducing the consumption of fuels, (ii) improving the efficiency of power plants, industrial facilities, and motor vehicles that generate CO₂ as a by-product, or (iii) capturing anthropogenic CO₂ at point of use.⁷ Theoretically, (i) can be accomplished by reducing the energy demand and shifting to alternative energy sources like solar, wind, and nuclear. Practically however, the transition to aforementioned alternative energy sources is difficult because these sources are not as abundant and cheap as fossil fuels such as coal. Option (ii), if pursued for coal-fired power plants, is estimated to cut CO₂ emissions from coal but only by about a mere 10-20%.⁸ Capturing CO₂ at point sources, as mentioned in (iii), remains the only feasible pathway which allows simultaneous reduction of CO₂ emissions and use of existing infrastructure to fulfill energy-related demands.⁷

Since CO₂ emission sources are vast in both number and nature, it is important to note that feasible targets for technological mitigation approaches are primarily stationary point sources where gases are emitted in concentrated streams and are thus viable for capture and

subsequent conversion if desired. Sources that are distributed in nature are extremely challenging, if not impossible, to combat effectively through abatement technologies. Industrial processes such as hydrogen production, natural gas processing, synthetic fuel production, and organic chemical production that release high purity and high concentration CO₂ waste gas streams yield the lowest CO₂ capture costs.⁹ All the aforementioned processes generate waste gas streams with CO₂ concentrations ranging between 30 - 100% by volume.⁹ Natural gas processing and synthetic fuel (coal-to-liquid (CtL)) production in particular can generate highly concentrated waste streams containing 95 - 100% CO₂ by volume. In contrast however, flue gas emissions generated by power plants, cement production, and iron and steel manufacturing processes contain relatively lower CO₂ concentrations as mentioned earlier which raises CO₂ capture costs as a result the additional expenses incurred upon gas separation prior to capture and storage. It is worth noting that even though high purity CO₂ off-gas producing industrial processes account for only 6% of total CO₂ emissions by all industrial sources combined, high concentration CO₂ streams are particularly appealing targets for carbon-capture based demonstration projects.⁹

1.2 CO₂ Electronic Structure as a Predictor of Reactivity

The major impediment to CO₂ mitigation and management is the stability of the kinetically inert CO₂ molecule. Consequently, considerable research efforts have thus far been devoted to discovering ways to enhance CO₂ reactivity for exploitation in CO₂ capture and conversion devices.

The challenge associated with CO₂ reactivity stems primarily from the fact that CO₂ is a linear, non-polar molecule containing carbon in its highest oxidation state, and is therefore

extremely thermodynamically stable ($\Delta H_f^0 = -393.52$ kJ/mol). However, despite of these challenges, the electronic structure of the CO₂ molecule presents several targets for reactivity. Possible reaction sites on the CO₂ molecule include (1) the electrophilic carbon atom, (2) the π -electron density of the double bonds, or (3) the lone pair of electrons on the oxygen atoms.¹⁰

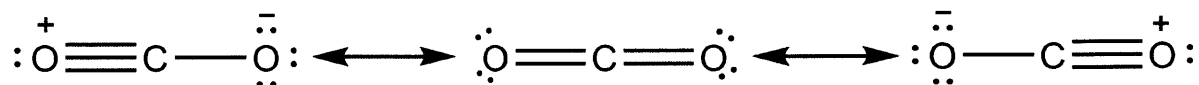


Figure 1-2: The three resonance structures of the linear CO₂ molecule.

To determine which of these three characteristic properties of the CO₂ molecule is most likely to enhance its reactivity, the electronic structure of the CO₂ molecule can be compared with that of the isoelectronic disulphide CS₂ molecule.¹¹ This comparison reveals that the lowest unoccupied molecular orbital (LUMO) of CO₂ has a lower energy level than that of CS₂, indicating a comparatively higher electron affinity (3.8 eV) of the carbon atom in the CO₂ molecule.⁸ On the other hand, the highest occupied molecular orbital (HOMO) of CO₂ has an energy lower than that of CS₂, which results in a high ionization potential (13.73 eV) and weak electron donating properties of CO₂ with respect to CS₂.⁸ These results strongly suggest that CO₂ is much more likely to be reduced than oxidized, and that the electrophilic, central carbon atom is of paramount importance in promoting the chemical activation and subsequent reactivity of the CO₂ molecule.

1.3 *Current CO₂ Mitigation Approaches*

CO₂ mitigation approaches can be broadly categorized into nearer-term solutions such as carbon capture and sequestration (CCS) technologies, and longer-term, prospective solutions, such as the conversion of CO₂ to either fuel-rich or solid phase products. This section

will present an overview of some key CO₂ abatement methods that have been previously demonstrated in literature.

1.3.1 *Carbon Capture and Sequestration (CCS) Technologies*

CCS is primarily concerned with the capture and long-term underground storage of CO₂. The CCS technologies discussed in this section utilize amines for CO₂ capture. Before the specifics of the technologies are described, a brief overview of amine chemistry is presented.

Amine Chemistry

Amines are nucleophilic organic compounds containing a basic nitrogen atom with a lone pair. They are essentially ammonia derivatives, where one or more of the hydrogen atoms is replaced with an organic group. Amines can be broadly categorized into primary (RNH₂), secondary (R₂NH) and tertiary (R₃N) depending on the number of hydrogens in ammonia that have been replaced. **Table 1-2** provides an example of each. ¹²


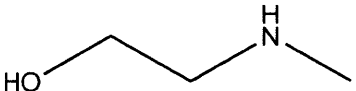
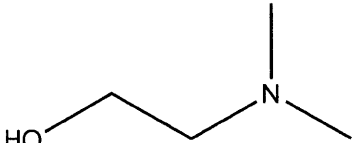
Type	Amine	pKa
Primary	 Monoethanolamine (MEA)	9.16
Secondary	 Methylaminoethanol (MAE)	9.40
Tertiary	 Dimethylaminoethanol (DMAE)	8.88

Table 1-2: Examples of primary, secondary and tertiary amines. The amine structure and pKa value corresponding to each type is provided.

Amine-CO₂ chemistry has been developed over several decades and has been extensively employed in various commercial, acid gas separation processes.¹³ Amines spontaneously bind to CO₂ via lone pair donation by the basic nitrogen atom of the amino group to the electrophilic carbon atom (C⁴⁺) of the CO₂ molecule. This results in the formation of a zwitterion, which is an overall neutral compound that contains positive and negative formal charges on different parts of its structure.¹³ For primary (RNH₂) and secondary amines (R₂NH), the zwitterion can undergo an *intramolecular* proton transfer to form carbamic acid (the proton gets transferred from the nitrogen group of the amine to one of the oxygen groups on the bound CO₂ within the same molecule). Alternatively, in the presence of an additional lean amine, the zwitterion may be converted to ammonium carbamate (RNH₃⁺RNHCOO⁻)

species through an *intermolecular* proton transfer, where the proton attached to the nitrogen group of the zwitterion is abstracted via lone pair donation by the nitrogen group of another basic amine molecule). **Figure 1-3** illustrates the mechanism of carbamate salt formation via a zwitterion upon reaction of two molecules of monoethanolamine (MEA), a primary amine, with one CO₂ molecule. The enthalpy of sorption is 82 kJ/mol at 40°C, and the corresponding CO₂ loading (mol of CO₂/mol of amine) is 0.5.¹⁴

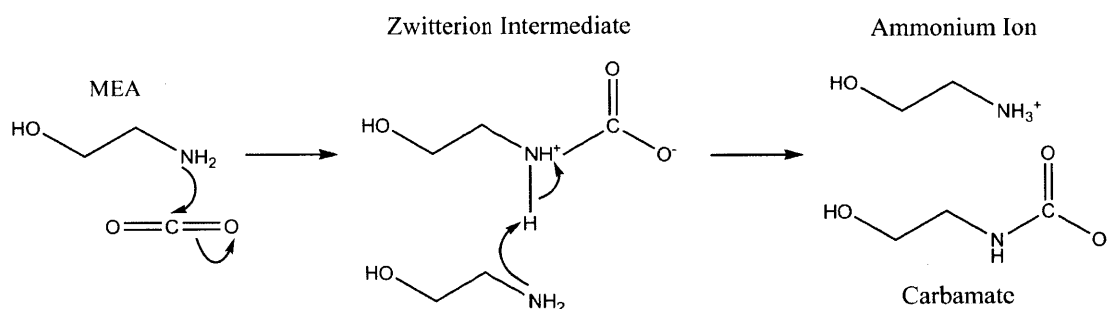


Figure 1-3: Mechanism of carbamate formation from the chemical absorption of 1 mole of CO₂ by 2 moles of a primary amine, MEA via a zwitterion intermediate.

Unlike primary and secondary amines, tertiary amines (R₃N) cannot form stable N-C bonds, nor generate stable carbamate products, because they do not have a transferrable proton attached to the nitrogen atom which can be abstracted by another basic amine molecule to form carbamate species. Tertiary amines can, however, accept a proton from carbonic acid, which is formed upon CO₂ dissolution in water, to form bicarbonates (HCO₃⁻). However, as this reaction consumes a water molecule, the use of tertiary amines for CO₂ capture is only viable in aqueous media.¹⁵ It is interesting to note that the CO₂ loading for tertiary amines (1 mol CO₂/amine) is higher than that observed for primary amines (0.5 mol CO₂/amine).

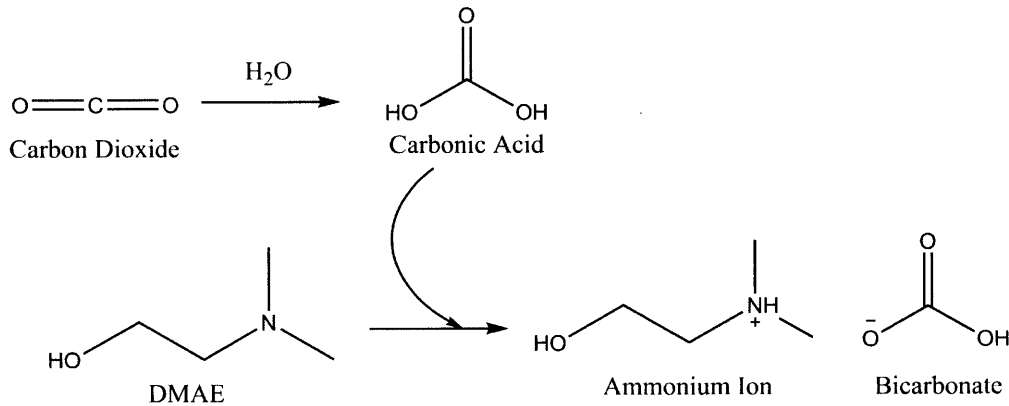


Figure 1-4: Formation of bicarbonate upon reaction of one mole of tertiary amine dimethylaminoethanol (DMAE) with one mole of CO_2 in water.

1.3.1.1 Thermal Amine Scrubbing

The current state of the art in carbon capture and sequestration technology is so-called thermal amine scrubbing, owing to process's selectivity towards CO_2 capture. In thermal amine scrubbing, an aqueous solution of an amine sorbent, typically monoethanolamine (MEA), is used to chemically absorb CO_2 from flue gas near ambient temperature in an absorber unit. The CO_2 -bound amine solution is then pumped to a desorber, where high temperatures (100-120 °C) are used to cleave the $-\text{N}-\text{C}-$ bond, upon which the CO_2 desorbs, and the amine is regenerated.¹⁶ At these temperatures, the enthalpy of desorption for MEA is 100 kJ/mol (compared to 82 kJ/mol at 40°C), which represents an energy penalty.¹⁴ The pure CO_2 released is compressed to pressures upwards of a 100 bars for geological sequestration, and the regenerated amine is fed back into the absorber where it can continue to rebind with CO_2 . A schematic depicting the physical process of thermal amine scrubbing is shown in **Fig.1-5**.

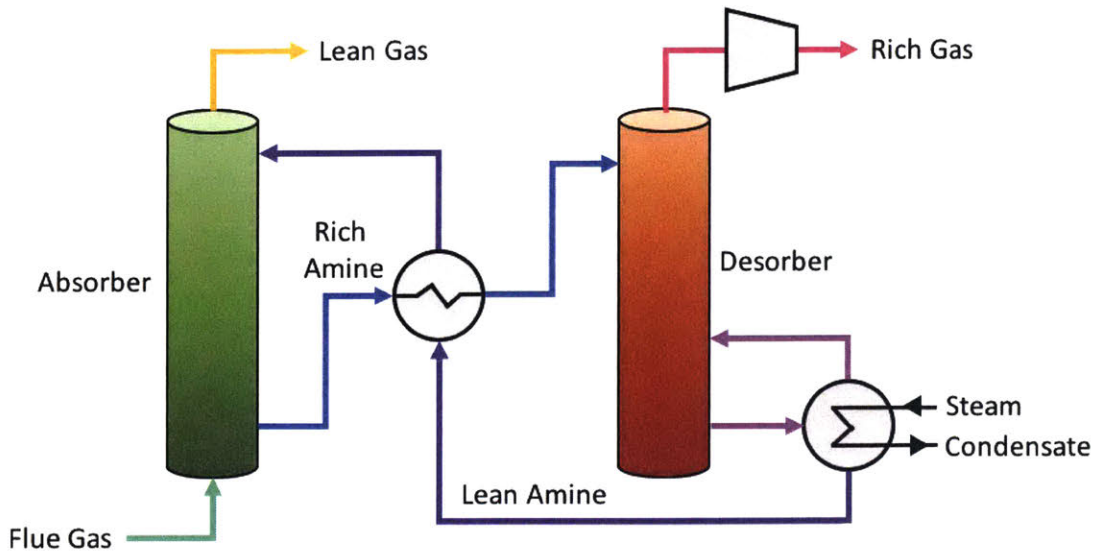


Figure 1-5: Schematic representation of a typical thermal amine scrubbing process.¹⁴

Thermal amine scrubbing has demonstrated considerable promise for use in post-combustion carbon capture from power plants and industrial facilities. According to the Global Carbon Capture and Storage Institute (GCCSI), as of 2016, there were around 38 commercial-scale CCS projects worldwide that are either operational, under construction or under planning.¹⁷ Particularly, 15 of these CCS projects were operational and had a combined CO₂ capture capacity of 30 million tons per annum. By the end of 2017, the number of operational large scale CCS projects is expected to rise to 21, with a total CO₂ capture capacity increasing to approximately 40 million tons per annum.¹⁷

While amine scrubbing is currently one of the most mature CCS technologies, the process has several drawbacks that continue to hinder its successful application at a large-scale. One of the main hurdles of conventional amine scrubbing is the energy intensiveness of the temperature-swing CO₂ desorption step, which typically requires high temperatures upwards of a 100°C. At these temperatures, competitive evaporation of water becomes dominant which parasitically consumes large amounts of energy, and adversely affects the overall thermal

efficiency of power plants that employ the CCS technology. Assuming 90% CO₂ removal efficiency, it is believed that the parasitic energy requirement for CO₂ desorption in the stripper, approximated to be around 0.19 to 0.28 MWh/ton CO₂,¹⁶ can reduce the power output of a typical plant by 20 to 30%.^{7,16,18} Additional challenges such as high energetic and logistical costs associated with compression transport and storage of CO₂, oxidative and thermal degradation of the amine, solvent loss by evaporation, amine corrosivity, and high viscosity of CO₂ adducts are also pervasive in traditional amine scrubbing systems.¹³

In order to address some of the shortcomings noted above, advanced amine systems exploring new chemistries are currently under investigation to reduce the energy consumption of the scrubbing process.¹⁸ One ongoing area of research largely revolves around identifying different types of amines with more optimal properties such as thermal and oxidative stability that are better suited for use in conventional amine scrubbing technologies.¹⁸ Despite of such developments however, the issue of solvent evaporation, which remains the leading cause of the parasitic energy requirement of the scrubbing process, is fundamentally difficult to overcome as a result of the aqueous nature of the medium in which CO₂ capture is most commonly accomplished.

1.3.1.2 Ionic Liquids for Carbon Capture

One alternative to aqueous CO₂ capture is exploring CO₂ capture chemistries in non-aqueous media such as ionic liquids.¹⁹ Ionic liquids are organic salts that are liquids at room temperature.²⁰ Room-temperature ionic liquids are attractive possible alternatives to water-based amine capture owing to the high solubility of CO₂ reported in these liquids, particularly imidazolium-based ILs.²¹ Previous studies have revealed that CO₂ interactions in imidazolium-based ionic liquids are dominated primarily by the anions like [BF₄]⁻, [PF₆]⁻, [Tf₂N]⁻ etc (see

Table 1-3).²² Such a finding might suggest that increasing the interaction strength of the anion by increasing its Lewis basicity might be one feasible approach to rationally tune the CO₂ solubility. Interestingly however, it was discovered that a higher basicity of the anion in the IL did not necessarily correspond to a higher CO₂ solubility in that IL. In fact, the highest CO₂ solubilities were obtained for ionic liquids with anions containing fluorinated alkyl chains, which indicates that CO₂ interactions with fluorinated alkyl chains on the anions and/or cations are considerably more important for boosting CO₂ solubility in ILs rather than acid/base interactions.²³

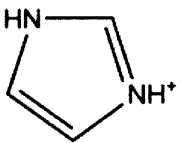
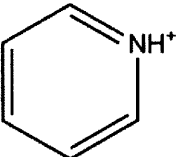
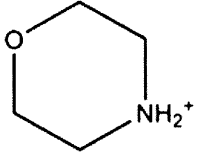
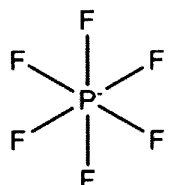
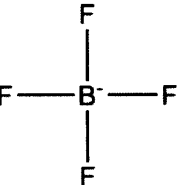
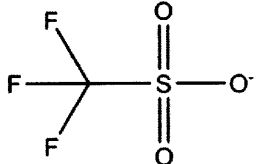
Common Cations	 Imidazolium	 Pyridinium	 Morpholinium
Common Anions	 Hexafluorophosphate	 Tetrafluoroborate	 Triflate

Table 1-3: Common cations and anions employed in ionic liquids used for CO₂ capture.²⁴

Furthermore, ionic liquids, in addition to physically absorbing CO₂ (non-covalent interactions), can also chemically complex with the gas (**Fig. 1-6**) through the formation of covalent bonds.²⁵⁻²⁷ Task-specific ionic liquids (TSILs) which commonly incorporate nucleophilic functional groups²⁸ such as the amino group (-NH₂) can chemically bind CO₂ and thus yield high CO₂ absorption capacities.²³ Such amine-functionalized ILs are not yet viable

for CO₂ capture however, owing to drastic increases in viscosities that are observed upon CO₂ complexation.^{29,30} To counteract this issue, researchers have proposed the design of designing ionic liquids with sufficiently nucleophilic anions that can complex directly with CO₂.³¹

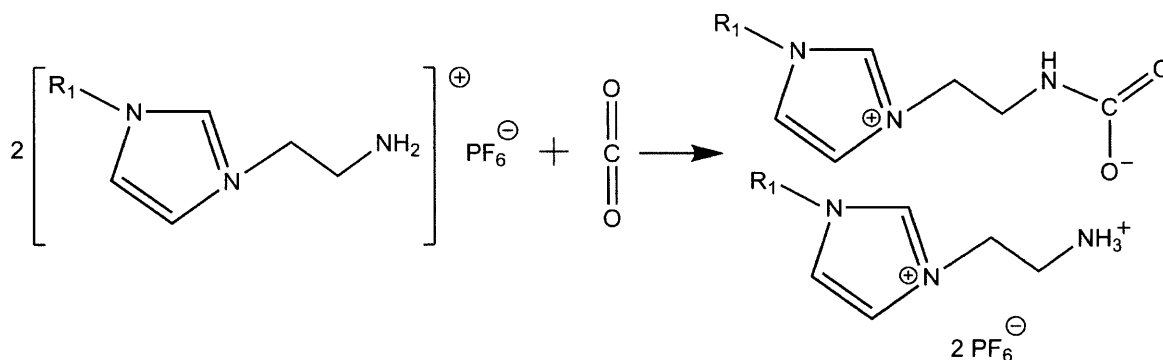
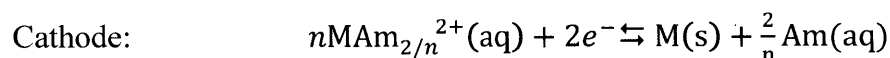
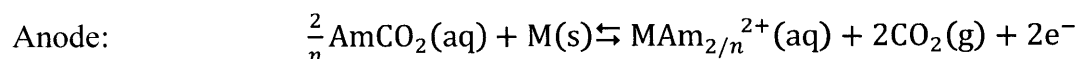
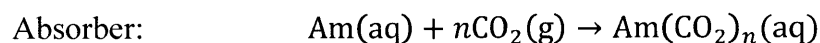


Figure 1-6: Reaction between an imidazolium-based ionic liquid and CO₂ to form carbamate.

Overall, ionic liquids present several advantages over aqueous amines, which include low volatility, high thermal stability, non-flammability, and chemical tunability.²⁰ The latter is especially promising for chemists working on molecular design for CO₂ capture, as it opens up new strategies to enhance both the chemical and physical absorption of CO₂, which is one viable route to improve the energetic metrics and operational lifetime of capture systems. In spite of this rich playground for designing new capture chemistries, however, ionic liquids remain prohibitively expensive. Moreover, the desorption of CO₂ and thermal regeneration is still energetically costly as in aqueous systems.³² Furthermore, the viscosity increases are up to 5 times more severe in ionic liquids than with conventional aqueous MEA, which can lead to large energetic penalties associated with pumping the fluids between components of the reactor.⁷

1.3.1.3 Electrochemically Mediated Amine Regeneration

In an effort to address the myriad challenges facing temperature-swing CO₂ desorption processes, a novel concept for amine regeneration - electrochemically mediated amine regeneration (EMAR) - was proposed by Stern et al. in 2013 as a potentially energetically-efficient alternative.² In an EMAR cycle, amines are regenerated electrochemically, rather than thermally, using metal cations that are generated at the anode, instead of heat, to displace CO₂ from the amine. Such an electrochemical approach for amine regeneration is a much more attractive alternative to thermal amine regeneration due to the ability of electrochemical processes to selectively attack target molecules, which in this case would be loaded amine species, instead of the entire medium.² In general, the EMAR process consists of three reactions that take place in the absorber, the copper-plated anode and the cathode respectively.²



In the above equations, Am represents an amine molecule, *M* represents the metal, and *n* represents the CO₂ loading i.e. the number of moles of CO₂ captured per mole of amine.³

In the EMAR cycle, ethylenediamine (EDA) is used as the CO₂ sorbent and copper is used as the redox responsive transition metal. EDA is a polyamine (i.e. an organic compound containing at least two primary -NH₂ groups) and was chosen specifically for the EMAR process due to its ability to form stable copper complexes which ensures a more thorough displacement of CO₂ from the amine-CO₂ complexes at the anode.² The reaction scheme for

the EMAR process utilizing EDA and copper is shown in **Fig. 1-7**, and the process can be described as follows.

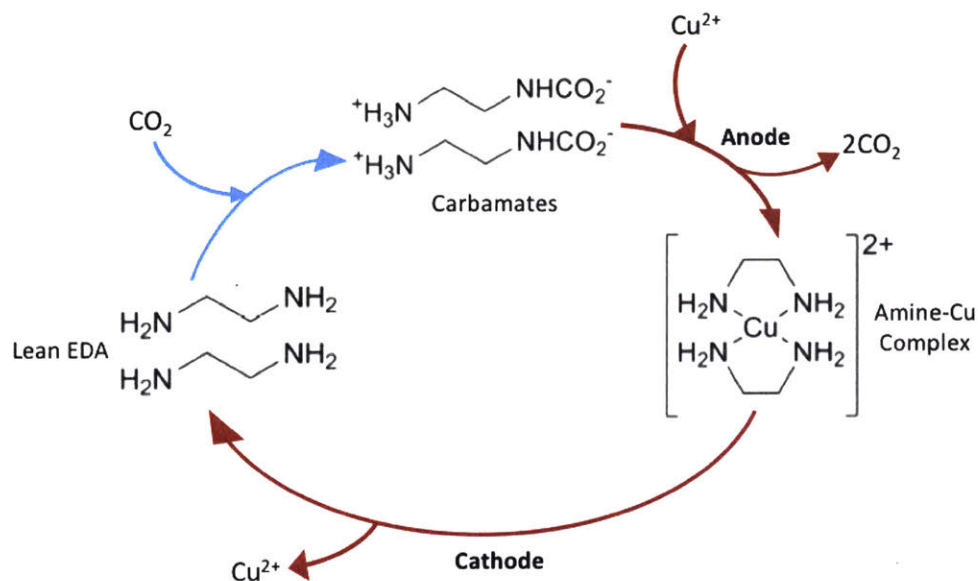


Figure 1-7: The EMAR cycle.¹⁴

Similar to traditional thermal amine scrubbing, the process begins by introducing CO₂-rich flue gas in an absorber containing an aqueous solution of lean ethylenediamine. This sorbent, which binds the CO₂ to form loaded amines or carbamates, is then pumped to the copper-plated anode of an electrochemical cell containing a predetermined concentration of a copper salt (e.g: CuNO₃, CuSO₄, or CuCl₂) and a supporting electrolyte typically composed of either a sodium or potassium salt.¹⁴ Upon oxidation of the metallic copper anode, cupric ions compete vigorously with the CO₂ for the amines, eventually displacing CO₂ entirely to form complexed amines. At the cathode, these complexed amines are reduced to regenerate amines in solution and form metallic copper at the cathode surface. The lean amines are then transported back to the absorber to complete the cycle, where they can continue to re-bind CO₂.

Bench scale demonstration of the EMAR process indicated that at optimal flow rates, 800 standard cubic centimeters per minute (sccm)/m² of CO₂ can be captured from 100kJ/mol of electricity.¹⁴ With reference to a completely reversible process, the maximum achievable thermodynamic CO₂ separation (Faradaic) efficiency of the EMAR process at open-circuit potential was around 70% for systems utilizing EDA.³ At ambient pressures, EMAR systems employing EDA could operate at 50°C and 70°C with 40% and greater than 50% CO₂ separation efficiencies respectively.¹⁴

As mentioned earlier, the EMAR process offers numerous advantages over the conventional thermal amine scrubbing technology. First, the EMAR regime's use of electricity rather than heat for amine regeneration largely reduces solvent loss by evaporation that is prevalent in thermal amine scrubbing systems. Second, the significantly greater stability of the Cu²⁺-amine complexes in comparison with just CO₂-amine complexes makes electrochemical cell operation at elevated pressures possible. This in turn allows for high pressure removal of CO₂ from the cell which drastically reduces costs incurred on downstream compression of CO₂.² Furthermore, the use of a relatively low cost polyamine like EDA also helps to reduce the absorber size and thus the associated capital costs because it can achieve comparatively higher CO₂ loadings for a smaller amount of polyamine solution.¹⁴

Despite of its several advantages over conventional CO₂ capture technologies however, the EMAR cycle still remains an electrolytic process requiring an energy input (~100 kJ/mol of CO₂ at room temperature)² for operation much like traditional scrubbing technologies.

1.3.2 *Electrochemical CO₂ Reduction*

The significant challenges of amine scrubbing have motivated considerable research into alternative approaches for CO₂ mitigation technologies. One such approach is the electrochemical reduction of carbon dioxide, which affords the possibility of converting CO₂ into potentially benign or even value-added products (reduced hydrocarbons such as CH₄, alcohols such as CH₃OH, syngas CO/H₂, or higher C₂ hydrocarbons) or chemicals.³³ In electrochemical CO₂ reduction, electron transfer instead of high temperatures are used for CO₂ activation and subsequent conversion. Electrochemical CO₂ reduction can be carried out in both aqueous and non-aqueous media with different outcomes, both of which are discussed below.

1.3.2.1 *Aqueous Electrochemical CO₂ Reduction*

In aqueous CO₂ reduction, CO₂ reduction (cathodic reaction) is coupled to a water oxidation reaction at the anode (to supply protons). From a thermodynamic standpoint, aqueous electrochemical reduction of CO₂ can yield a number of potential energy-rich products at moderate reduction potentials (within several hundred mV of 0 V vs. NHE),^{34,35} the most significant of which are listed in **Table 1-4**. Amongst this list, the most energy dense those that contain carbon in their most reduced form or alternatively, those in which the C-O bond is cleaved. Even though experimental investigations on aqueous electrochemical CO₂ reduction have thus far reported high Faradaic efficiencies (> 90 %) for some products like formic acid (HCOOH) and carbon monoxide,³³ selectivity towards more reduced products remains a major challenge.

Half-Cell Cathodic Reaction	E^0 (V vs NHE)	O.S. of C
$\text{CO}_2 + \text{H}^+ + 2\text{e}^- \rightarrow \text{HCOO}^-$	-0.225	+2
$\text{CO}_2 + 2\text{H}^+ + 2\text{e}^- \rightarrow \text{CO} + \text{H}_2\text{O}$	-0.103	+2
$2\text{CO}_2 + 12\text{H}^+ + 12\text{e}^- \rightarrow \text{C}_2\text{H}_4 + 4\text{H}_2\text{O}$	0.079	-2
$\text{CO}_2 + 8\text{H}^+ + 8\text{e}^- \rightarrow \text{CH}_4 + \text{H}_2\text{O}$	0.169	-4
$2\text{H}^+ + 2\text{e}^- \rightarrow \text{H}_2$	0.00	N/A

Table 1-4: Possible CO_2 reduction reactions in aqueous media. The provided potentials have all been measured on the copper electrode.³⁴ The oxidation state of carbon is denoted by O.S. in the above table.

In aqueous media, there are two primary challenges associated with CO_2 reduction: (a) the large thermodynamic barrier that exists because of the endothermicity of the full cell reaction (the potential of the anodic, water splitting reaction is higher than that of formation of fuel-rich products at the cathode), and (b) the large kinetic overpotential (-1.9 V vs. SHE) of the single electron transfer step which converts a linear CO_2 molecule to the bent CO_2^- anion radical.^{36,37} Due to the significantly high kinetic overpotential incurred upon the reduction of CO_2 to form the reaction intermediate CO_2^- , suitable electrocatalysts that can stabilize the intermediate and consequently minimize the energy input for the CO_2 reduction process in aqueous electrolytes have been the subject of extensive experimental investigation.³⁸⁻⁴¹ In fact, past literature has indicated that adsorbing the CO_2 anion radical on a catalyst surface can lead to an approximate 0.3 V decrease in overpotential upon the first reduction step in aqueous electrolytes.³³

Advances in Electrocatalysis for Aqueous CO_2 Reduction

To address the prohibitively large kinetic overpotentials incurred upon the first electron transfer step in CO_2 reduction, researchers have been identifying suitable metal catalysts that facilitate the rate limiting step by adsorbing, and therefore bending the CO_2 molecule on their

surface. If CO₂ is adsorbed on a metallic catalytic surface prior to reduction, there are two main ways according to which the CO₂ conversion reaction can proceed following the formation of the adsorbed CO₂ anion radical- one is the formation of formate and the other is the formation of carbon monoxide or further reduced hydrocarbons via adsorbed CO on the surface.^{42,43}

Ab-initio modeling suggests that metals that have intermediate CO_{ads} –surface bond strengths are ideal candidates for CO₂ reduction catalysts.³³ However, note that because of the aqueous environment of the reduction process, the hydrogen evolution reaction (HER) is the main competing reaction to CO₂ reduction at the positive electrode.³⁴ Therefore, ideal catalysts for aqueous CO₂ reduction not only require intermediate adsorbate-surface bond strengths as suggested by the Sabatier principle,³³ but should also possess high overpotentials for HER. A wide range of metal electrodes have been explored as potential catalysts for aqueous CO₂ reduction and results from several experimental investigations are summarized below.⁴²

Electrode Material	η for HER	CO Adsorption Strength	Most Reduced Product
Hg, Cd, Pb, Sn	High	Weakest	Formate
Pt, Ni, Fe, Ti	Low	Strong	Hydrogen
Au, Ag, Zn	Medium	Intermediate	Carbon Monoxide
Cu	Medium	Intermediate	Hydrocarbons

Table 1-5: Properties of electrode materials that have been previously investigated in literature for their catalytic behavior in aqueous CO₂ reduction.⁴²

As shown in the **Table 1-5**, metal electrodes such as Hg, Cd, Pb etc. have large overpotentials for HER with minimal CO absorption strengths, and therefore yield formate as the primary product.⁴² However, because the formation of formate does not involve the

breaking of the C-O bond, these metals are not effective for catalyzing CO₂ reduction to produce energy-rich products. On the other hand, metals like Pt, Ni and Fe result in very strong CO_{ads}-surface bonds upon CO₂ reduction.⁴² These tightly bound adsorbates on the metal surface are detrimental to catalyst performance because they block the majority of the active sites on the catalyst surface, thereby causing catalyst poisoning. In addition to this, their low overpotentials for HER result in hydrogen as the primary product upon CO₂ reduction, which is highly undesirable. Medium hydrogen overpotential electrodes such as Ag, Au, Zn and Cu with intermediate CO adsorption strength are much more promising catalysts for CO₂ reduction.⁴² Amongst these, metals like Au, Ag and Zn can enable the adsorbed CO species to desorb to form carbon monoxide, whereas as Cu allows further reduction of CO_{ads} to hydrocarbon fuels, albeit with low efficiencies.²⁴ The possibility of forming fuel-rich products from aqueous electrochemical CO₂ reduction with the use of copper electrodes has established copper metal as one of the most widely employed electrocatalysts for CO₂ reduction.

Despite of the progress made with regards to identifying copper metal as a suitable catalyst however, the kinetic limitations of the electrochemical CO₂ reduction process remain severe, such that reactions must be driven at high overpotentials (~ 1 V) to obtain significant yields and selectivity for reduced products. Another aspect to note is that aqueous electrochemical reduction of CO₂ is an *electrolytic* process i.e. the reduction process is electrically driven. Therefore, it is imperative that the energy required for the electroreduction of CO₂ also comes from renewable energy sources if the process is to successfully mitigate CO₂ emissions.

1.3.2.2 Non-Aqueous Electrochemical CO₂ Reduction

To address the limitations of aqueous CO₂ reduction, one alternative is to shift to nonaqueous (organic) electrolyte systems, which permits the use of highly reducing alkali/alkaline earth metals (Li, Na, Ca, Mg) that yield large thermodynamic driving forces for the conversion of CO₂ to much more stable products such as carbonates and oxalates.⁴⁴⁻⁴⁶ Moreover, the large voltage window afforded by the use of nonaqueous electrolytes⁴⁷ is not only beneficial for probing chemical activity of CO₂ over a large energy range, but also allows access over a wider range of reaction pathways. Owing to the absence of protons, the end-product in nonaqueous systems is typically Li₂CO₃ or other mineral solids^{45,46,48} rather than a fuel. The value-added component of such a metal-CO₂ configuration is not the chemical end product but rather electricity, which can be used to achieve CO₂ emissions reductions while offsetting additional energetic costs in the plant.

In addition to this, the solubility of CO₂ is also significantly higher in nonaqueous solvents than it is in aqueous media. (see **Table 1-6** below) Gas solubility in conventional, aprotic battery solvents is of crucial importance in non-aqueous, metal-gas electrochemical systems due to its profound impact on cell performance.⁴⁹ **Table 1-6** lists CO₂ solubilities in a wide range of solvents under standard conditions (298 K and 1 atm). As evident from the table, the solubility of carbon dioxide, a non-polar gas, is not only far greater in organic solvents like DMSO (dielectric constant, $\epsilon = 48$) as opposed to that in water ($\epsilon = 80.4$), but also well exceeds the target solubility (~1-10 mM) defined by the solubility of oxygen in the well-established Li-O₂ system.⁵⁰

Solvent	Solubility/mM
Tetraglyme (TEGDME) ⁵¹	111
Propylene Carbonate (PC) ¹⁰	140
Dimethylsulfoxide (DMSO) ¹⁰	135
Tetrahydrofuran (THF) ¹⁰	211
N,N-dimethylformamide (DMF) ¹⁰	175
Acetonitrile (ACN) ¹⁰	280
Methanol ⁵¹	138
Water ⁵¹	34

Table 1-6: CO₂ solubility in select organic solvents at 298 K and 1 atm.

Another prominent advantage of non-aqueous electrochemical CO₂ reduction in metal-gas systems, as mentioned earlier, is that it offers the possibility of converting gas-phase CO₂ into solid-phase products. **Table 1-7** lists some possible cell reactions involving non-aqueous CO₂ reduction with lithium metal and the associated thermodynamic parameters. As shown in the table below, the formation of solid phases like Li₂CO₃ and carbon (C) are the most thermodynamically favorable.

Overall Cell Reaction	ΔG^0 (kJ/mol)	n	E^0 (V)
$\text{CO}_2 + 2\text{Li} \rightarrow \text{CO} + \text{Li}_2\text{O}$	-305	2	1.58
$2\text{CO}_2 + 2\text{Li} \rightarrow \text{Li}_2\text{CO}_3 + \text{CO}$	-481	2	2.49
$\text{CO}_2 + 4\text{Li} \rightarrow \text{C} + 2\text{Li}_2\text{O}$	-730	4	1.89
$3\text{CO}_2 + 4\text{Li} \rightarrow 2\text{Li}_2\text{CO}_3 + \text{C}$	-1081	4	2.80

Table 1-7: Possible CO₂ reduction reactions in non-aqueous, lithium based systems. The thermodynamic parameters associated with each reaction are provided.

Converting CO₂ to benign solids that conveniently grow on the positive electrode over the course of discharge makes subsequent storage of the solid-phase product potentially safer. In traditional CCS technologies that employ geologic sequestration, CO₂ is compressed to a supercritical fluid with a density ranging between 0.6-0.8 g/cm³, and injected to depths of at

least 1 km underground to an appropriate storage site.⁵² In addition to the high costs associated with the sequestration process, there is a risk of potential atmospheric or subsurface leakage of CO₂ from storage sites, which can not only cause serious environmental harm but can also have detrimental effects on human and animal health.⁵² The conversion of CO₂ to solid phase products which have densities close to an order of magnitude higher (see **Table 1-8**) than that of supercritical CO₂ helps eliminates this risk of leakage.

Product	Density (g/cm³)
Li ₂ CO ₃ (<i>s</i>)	2.11
Li ₂ O (<i>s</i>)	2.01
C (<i>s</i>)	2.25
CO ₂ (<i>l</i>) ⁵²	0.6

Table 1-8: Mass densities of potential products that can be formed from the electrochemical reduction of CO₂ in either aqueous or non-aqueous media. The density for CO₂ (*l*) corresponds to T = 30°C and P = 8 MPa.⁵²

Previous literature has shown, however, that CO₂ is generally inactive in nonaqueous based electrolytes, yielding poor conversion kinetics.⁴⁵ The reason behind the electrochemical inactivity of CO₂ in pure Li-CO₂ batteries is once again the extremely large overpotentials incurred upon the first electron transfer step that converts the linear CO₂ molecule to the bent CO₂⁻ anion radical.³³ The conversion of CO₂ has mainly been demonstrated in non-aqueous Li-air batteries where CO₂ is employed as a contaminant.^{45,46,53} In Li-O₂/CO₂ batteries, CO₂ is not directly electrochemically activated, but is rather *chemically* activated via a reaction with the electrochemically generated oxygen anion radical species O₂⁻.^{45,54}

Non-aqueous CO₂ reduction has also been demonstrated in ionic liquids (ILs),⁴⁴ where CO₂ is electrochemically reduced in the presence of Li⁺ ions to form Li₂CO₃ and carbon, with Li₂CO₃ being the primary discharge product.²⁹ However, because ILs are inherently very

viscous in nature, the electrochemical cells need to be operated at higher temperatures (60-100°C) to reduce transport barriers and attain optimal cell performance.⁴⁴

1.4 Combined Chemical-Electrochemical CO₂ Capture and Conversion

In this work, we report a combined chemical-electrochemical device for post-combustion capture and subsequent conversion of CO₂ into a benign, solid alkali metal-containing phase (lithium carbonate, Li₂CO₃) at low overpotentials. The developed system employs an amine, e.g. 2-ethoxyethylamine (EEA) as used herein, in an organic electrolyte (e.g. dimethyl sulfoxide (DMSO)) to bend the CO₂ molecule via chemisorption prior to electrochemical reduction at a simple carbon electrode in a Li-CO₂ battery configuration. The chemical absorption step bends the CO₂ molecule through formation of an N-C bond by forming an adduct, and delivers this adduct to the electrode surface for electron transfer (**Fig. 1-8**). In doing so, this molecular “pre-activation” step chemically facilitates bending of the CO₂ *before* electron transfer occurs, and therefore modifies the reaction energetics by overcoming the conventional rate-limiting step in classical electrochemical CO₂ reduction. This provides an alternative approach to both conventional, aqueous-based amine capture systems (capture followed by regeneration), and to state of the art Li or alkali metal-CO₂ batteries (direct CO₂ electroreduction).

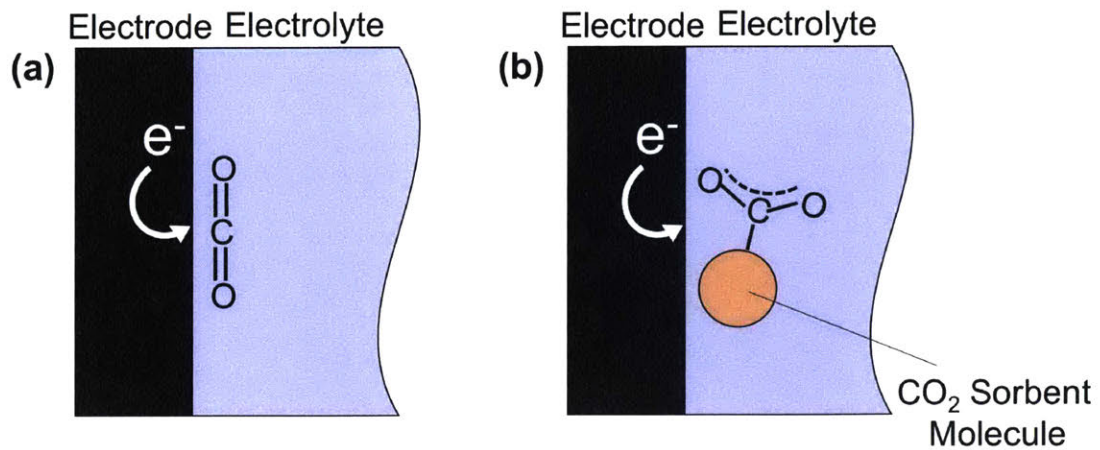


Figure 1-8: Schematic comparing the proposed approach (b) with the classically employed approach (a) for CO₂ reduction.

2 EXPERIMENTAL DETAILS

Li-CO₂ Cell Assembly - Li-CO₂ electrochemical cells were constructed using Swagelok components inside an argon-filled MBraun glovebox with oxygen and water content below 0.1 ppm. A 10 mm diameter Li metal disc (0.38 mm thickness, Sigma Aldrich) that was pre-stabilized by a several-day soak in 0.1 M LiClO₄ in propylene carbonate (>99%, Sigma Aldrich) prior to use in the cell was used as the negative electrode, a 13 mm diameter disc of Whatman QM-A quartz filter was used as the separator (2.2 μm pore size, 450 μm in thickness, Sigma Aldrich), Vulcan carbon (VC) loaded onto a Celgard separator (12 mm in diameter) was used as the positive electrode, and 75 μL of 0.3 M LiClO₄ in DMSO containing a known concentration of CO₂-bound EEA was employed as the electrolyte. The cells were assembled in the following manner (see **Fig. 2-1**) : (a) Li foil anode was pressed onto the stainless steel current collector; (b) a 13 mm Whatman separator was placed over the Li metal and 50 μL of electrolyte was added; (c) the VC carbon positive electrode was placed with the coated side facing outwards towards the gas inlet and 25 μL of electrolyte was added; 5) a 316 stainless steel mesh (0.5 inches in diameter) was placed over the cathode and stainless steel spring was added over top. Once the cells were assembled, they were purged with CO₂ for 50 seconds, pressurized to 1.4 bars, and sealed within the glovebox for discharge testing outside the glovebox. Following a rest step for 15 hours, the cells were discharged galvanostatically over a range of current densities at room temperature to a cutoff potential of 2 V vs. Li. All electrochemical testing was performed using a Biologic VMP3 potentiostat.

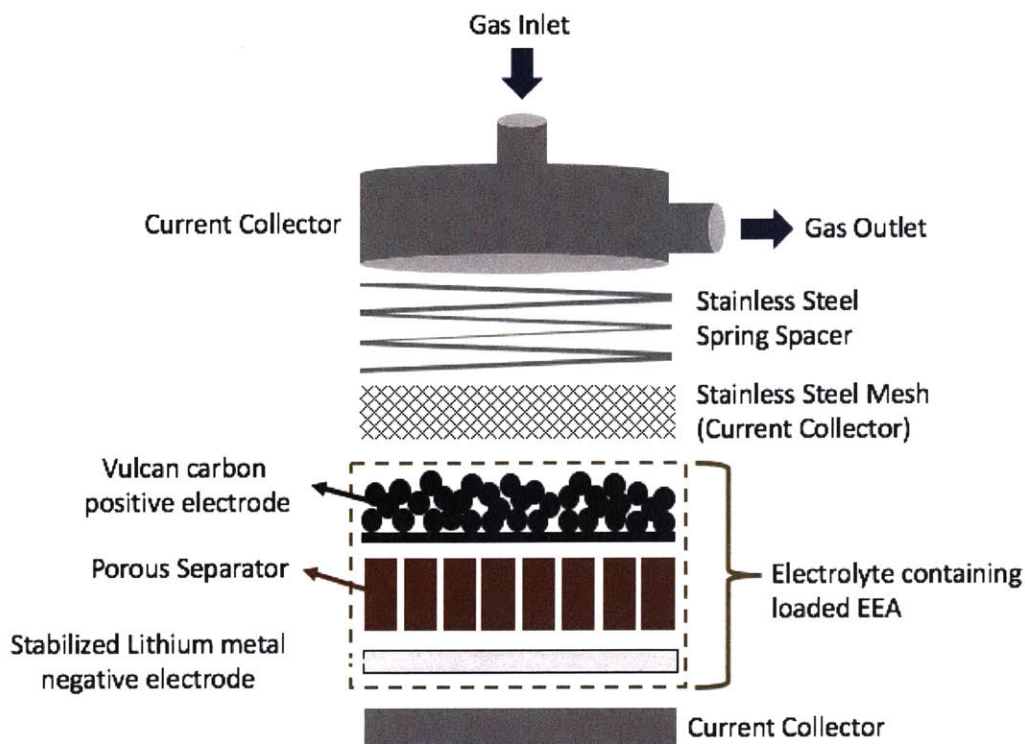


Figure 2-1: Schematic representation of an Li-CO₂ Swagelok cell.

Positive Electrode Preparation - The porous positive electrode was prepared by uniformly coating a sonicated ink composed of Vulcan Carbon (VC, XC72), isopropanol, and lithiated Nafion (LITHion dispersion, Ion Power, USA) with a Nafion/VC weight ratio of 0.5/1 onto a sheet of Celgard separator (Celgard 480, 25 μm thickness). After air-drying the VC coated Celgard at room temperature, 12 mm diameter electrode discs were punched out and subsequently dried for 24 hours under active vacuum in a glass oven (Buchi) at 70 $^{\circ}\text{C}$. The electrodes had a carbon loading ranging from $0.48 \pm 0.13\text{mg}$ ($0.36 \pm 0.10 \text{mg}/\text{cm}^2$) and an average thickness of around 15 μm . The specific surface area of the Vulcan carbon electrodes in general was around $100 \text{m}^2/\text{g}$.⁵⁵

Electrolyte preparation – The electrolyte used in this study consisted of 0.3 M LiClO₄ in DMSO with an amine additive. Dimethyl sulfoxide (DMSO, > 99.9%) and lithium perchlorate (LiClO₄) salt (Battery grade, 99.9% metal basis) were purchased from Sigma Aldrich, and 2-ethoxyethylamine (EEA, CAS Registry Number 110-76-9, 99%, TCI) was purchased from Fisher Scientific. Prior to use, LiClO₄ salt was dried for 24 hours under active vacuum in a glass oven (Buchi) at 70 °C and was transferred to the glovebox without exposure to ambient. DMSO was dried over fresh molecular sieves (Type 3Å, Sigma Aldrich) inside the glovebox for at least 24 hours at room temperature. The molecular sieves had been previously dried under active vacuum in a glass oven at 120 °C for a minimum of 24 hours prior to being taken inside the glovebox. The amine was stored inside the glovebox and was used as purchased.

Every time a batch of Li-CO₂ cells was assembled, a small volume (~500 µL) of 0.3 M LiClO₄ in DMSO was transferred to a flask and a pre-determined amount of EEA was added. The electrolyte containing the amine additive was then purged with CO₂ for ~ 20 seconds prior to its introduction into the electrochemical cell to prevent any parasitic reaction between the lean EEA and the Li metal anode.

Cyclic Voltammetry - Electrochemical measurements were conducted using a 3 electrode electrolysis-type cell containing Li foil or Pt wire as the counter electrode, a nonaqueous AgNO₃ reference electrode (Ag wire immersed in 0.1 M TBAClO₄ / 0.01 M AgNO₃ in acetonitrile, calibrated against a Li metal electrode in 3 mL of 0.3 M LiClO₄ in DMSO (0 V vs. Li/Li⁺ = -3.700V vs. Ag/Ag⁺)), and a carbon cloth (1071 HCB, Fuel Cell Store) or glassy carbon (GC, Pine, 0.196 cm²) mounted to a Modulated Speed Rotator (Pine) as the working

electrode in a hermetically sealed Mbraun glovebox. Prior to each set of measurements, the GC electrode was polished using 5 μm , 3 μm , 1 μm , and 0.3 μm polishing papers (Thor Labs) to a mirror-finish, followed by sonication in de-ionized water (18.2 M Ω cm, Millipore) water for several minutes and drying under active vacuum in a glass oven (Buchi) at 70 °C for at least 12 hours. The carbon cloth electrodes on the other hand were vacuum dried for 24 hours in a glass oven (Buchi) at 120 °C. Both types of positive electrodes were transferred directly into the glovebox without exposure to the ambient.

Prior to cell assembly as shown in **Fig. 2-2**, the potential of the reference electrode relative to Li/Li⁺ was measured by immersing a piece of Li foil in pure electrolyte solution (0.3 M LiClO₄ in DMSO) without any amine or CO₂, and monitoring the potential of Li metal vs. Ag/Ag⁺ for approximately 20 minutes until the potential stabilized. At that point, the potential difference between the reference electrode and Li/Li⁺ was measured, and was typically found to be around $0 V_{\text{Li}} = -3.69 \text{ V vs. Ag/Ag}^+$, which is in good quantitative agreement with the value published in literature.⁵⁶ Next, the working electrode was immersed in the electrolyte and steady state CVs were obtained in an argon headspace by scanning the working electrode potential from 1 – 3 V vs. Li at a scan rate of 20 mV/s.

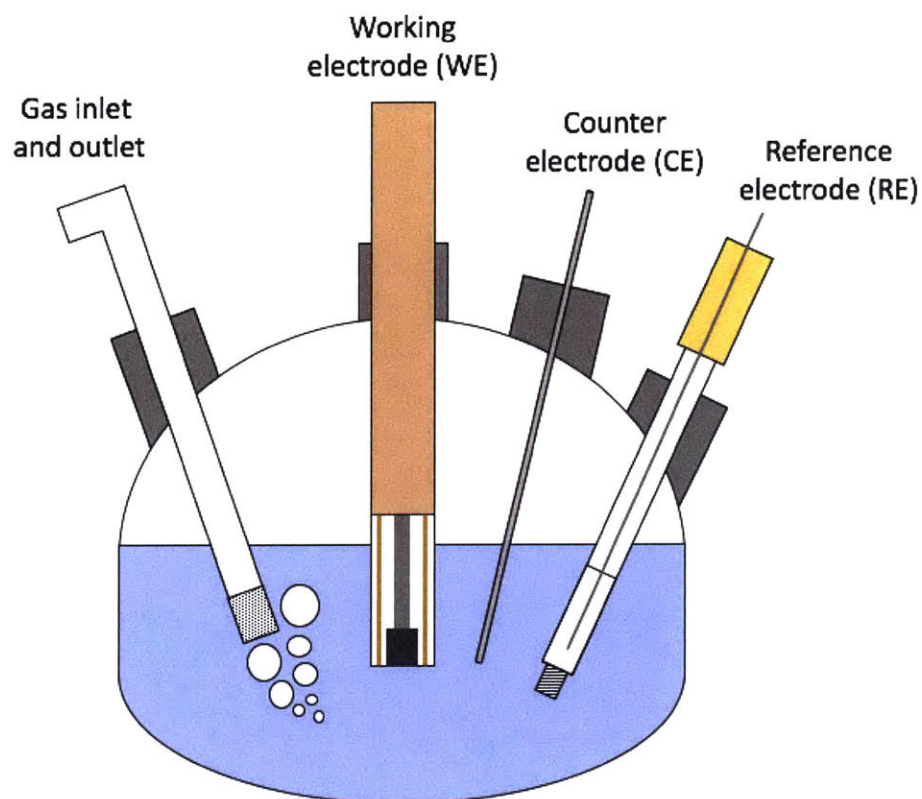


Figure 2-2: Schematic representation of a three-electrode electrolysis type cell.

A known concentration of lean EEA (no CO_2) was then added to the electrolyte and the solution was purged with CO_2 for 15 minutes, after which the ports of the glass cell were sealed and the solution was allowed to rest for least three hours to allow for Li ions to exchange with protons on the ammonium carbamate species ($\text{RNH}_3^+\text{RNHCOO}^-$) to form the electrochemically active lithium carbamate. Following this rest step, the potential of the working electrode was scanned from 1 - 3 V vs. Li/Li^+ at a scan rate of 20 mV/s. It is worth noting that the potential of the reference electrode relative to Li/Li^+ did not vary significantly upon the addition of amine in the electrolyte and the subsequent CO_2 purge.

Discharge Product Characterization

Scanning Electron Microscopy (SEM) - Following discharge, Li-CO₂ cells were disassembled inside the glovebox and the cathode was washed in DMSO and dried under Ar prior to SEM imaging. To minimize exposure to ambient, the sample was sealed in a glass vial under Argon inside the glovebox and was quickly transferred (< 1 min) to the SEM chamber before imaging. All images were collected using a Zeiss Merlin High-resolution SEM operating at an accelerating voltage ranging of 3 kV and beam current of 82 pA.

Infrared Spectroscopy – After a DMSO rinse and subsequent drying under Argon, discharged cathodes were sealed in glass vials inside the glovebox and transferred outside for FTIR measurements on a Nicolet 6700 FT-IR spectrometer (Thermo Scientific). All measurements were performed in the transmission mode over a wavenumber range of 650 to 4000 cm⁻¹ by ATR using either a Germanium (Ge) or a Zinc Selenide (ZnSe) crystal depending on the sample under consideration. “Dark” samples such as carbon positive electrodes were analyzed exclusively using the Ge crystal.

¹³C and ¹H NMR – ¹³C and ¹H NMR measurements were performed using a Varian Mercury 300 MHz NMR spectrometer equipped with a 5 mm PFG (pulsed field gradient) quad probe. All samples were prepared using an appropriate quantity and type of deuterated solvent (DMSO-d₆ or D₂O (Sigma Aldrich)) inside the glovebox. A small sample volume (700 μL) was then drawn and transferred to a capped Wilmad NMR tube (528-PP-7) for NMR analysis.

Gas Chromatography (GC) - GC measurements were performed on an SRI 8610C Gas Chromatograph (SRI Instruments) equipped with FID and TCD detectors. For calibration purposes, two separate gases were initially run, one containing 0.5% hydrogen and 0.5% carbon monoxide in a nitrogen carrier gas and a second one containing 1% methane in an argon carrier gas. Once the calibrations were performed, 100 μ L of gas from the discharged cell's headspace was drawn using a syringe and manually injected into the GC inlet for analysis.

X-Ray Diffraction - For XRD analysis, 12mm diameter discs of Toray paper 030 (FuelCellsEtc) were used as the positive electrodes. XRD spectra were obtained for both the pristine and discharged electrodes using a PANalytical X'Pert Pro with a copper anode ($\text{Cu K}\alpha$). An air-sensitive sample holder was used to seal the discharged electrode under an Argon environment inside the glovebox to prevent atmospheric contamination during measurements. All scans for discharge product detection were performed from $10^\circ < 2\theta < 90^\circ$ at a typical scan rate of $0.4^\circ/\text{min}$. Note that for XRD analysis, Toray carbon paper (FuelCellsEtc, TGP-H-030) was used as the positive electrode because the characteristic XRD peaks of this material had minimal overlap with those of crystalline lithium carbonate.

Quantification of Li_2CO_3 yield - Discharged cathodes (GDL) retrieved from Li- CO_2 cells were rinsed with DME and were left to dry under Argon for several hours inside the glovebox. Once dry, the samples were taken outside the glovebox and a predetermined quantity of deuterium oxide (D_2O , Sigma Aldrich > 99.9%) containing 0.3 M H_3PO_4 was added directly to the discharged cathodes. A standard for calibration was obtained in a similar manner by separately preparing a 20 mM Li_2CO_3 (Sigma Aldrich, 99.997%) solution in D_2O containing 0.3 M H_3PO_4 .

The acid was added to aid dissolution of Li_2CO_3 in D_2O . 1 mL of all solutions containing dissolved lithium carbonate were transferred to capped NMR tubes for NMR analysis. Quantification of lithium carbonate formed upon discharge was performed by ^7Li NMR on Varian Inova 500 MHz NMR spectrometer equipped with dual broadband radio frequency (RF) and a 5 mm variable temperature VT switchable PFG probe.

3 RESULTS

3.1 Electrolyte Design

Amines are typically used in aqueous-based CO₂ capture chemistry and therefore a significant aspect of this project was the translation of aqueous amine chemistry to nonaqueous (aprotic) battery electrolyte systems. Using arbitrary amines (with labile protons) in alkali metal systems would conventionally be considered challenging owing to the possibility of evolving H₂ gas, which represents a parasitic consumption of the amine. To ensure that amine chemical functionality could be successfully retained in a nonaqueous environment, we first investigated the chemistry of CO₂ uptake by amines in nonaqueous media.

3.1.1 *Products of Amine-CO₂ Complexation in Non-Aqueous Electrolytes*

The chemistry of CO₂ uptake by monoethanolamine (MEA) and 2-ethoxyethylamine (EEA) was first investigated in two organic solvents, namely TEGDME and DMSO as a preliminary screen for electrochemical reaction viability. TEGDME and DMSO were chosen as the candidate electrolytes because they have previously demonstrated promise in well-established electrochemical metal-gas systems like Li-O₂⁵⁷⁻⁵⁹ and Li-CO₂ batteries.^{44,60,61} As for the candidate amines, EEA was selected as a result of its higher solubility in organic solvents¹² and MEA was chosen because of its low cost and commercial significance in traditional amine scrubbing technologies.


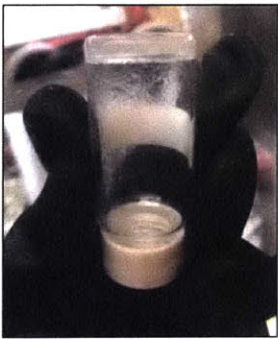
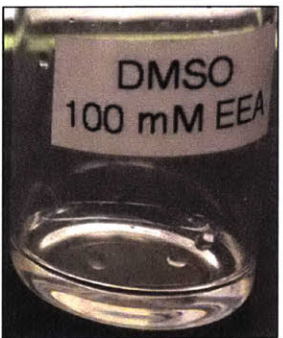
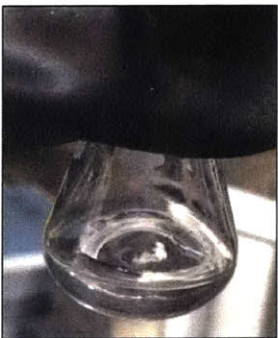
Solvent	Solvent with 0.1 M CO ₂ -bound EEA	Solvent with 0.3 M LiClO ₄ and 0.1 M CO ₂ -bound EEA
TEGDME		
DMSO		

Table 3-1: Photographs of electrolyte or solvent samples containing complexed amine species indicating the feasibility of DMSO for use in this system.

To determine the feasibility of the use of amines as CO₂ sorbents in non-aqueous media, 0.1 M amine was introduced into 1 mL of the chosen solvent or electrolyte. The solution was subsequently purged with CO₂ for approximately 20 seconds and allowed to rest for ~ 24 hours. A piece of lithium metal was then added to the solution to check for lithium stability in the presence of complexed amine species within the electrolyte. MEA was observed to react instantaneously in the presence of Li metal, which corresponded to the observable liberation of hydrogen gas. The source of this parasitic reactivity was attributed to the –OH terminal group of MEA. Similarly, for EEA, the introduction of CO₂ gas in a solution containing 0.1 M EEA in 0.3 M LiClO₄ in TEGDME resulted in the formation of a highly viscous, gel-like substance (**Table 3-1**), rendering TEGDME impracticable for use with EEA in a battery electrolyte. The

addition of CO₂ gas in 0.3 M LiClO₄ in DMSO containing 0.1 M EEA, however, initially yielded a clear solution (**Table 3-1**), which eventually showed signs of precipitation over the course of several days. The absence of precipitates from the solution containing complexed EEA species in pure DMSO (no salt) indicates that LiClO₄ is responsible for precipitation in the electrolyte (**Fig. 3-4**). In the remainder of this section, the electrolyte employed is always 0.3 M LiClO₄ in DMSO containing 0.1 M EEA, unless otherwise noted.

3.1.1.1 Products of EEA-CO₂ complexation in DMSO

To understand the precipitation process in the electrolyte, the composition of products formed upon CO₂ complexation with 50 mM EEA in pure DMSO-d₆ were examined using ¹H NMR. The rationale behind choosing 50 mM as the amine concentration was to prevent shimming problems, which can occur in NMR measurements when solutions are too concentrated. **Figure 3-2** shows the proton NMR spectra of (a) lean EEA and (b) loaded amine. The ¹H NMR resonance associated with the amino group of the lean amine i.e. CH₃CH₂OCH₂CH₂NH₂ was initially observed at 1.3 ppm vs TMS. Upon introduction of CO₂ into the electrolyte containing 50 mM of lean amine, the –NH₂– peak shifts downfield and splits into two peaks at 6.6 and 10.2 ppm to form an equilibrium mixture of carbamic acid and carbamate species.¹² The resonance at 6.6 ppm represents the –NH– protons of the carbamate and carbamic acid species, whereas the peak at 10.2 ppm corresponds to the –COOH protons of carbamic acid that are in fast exchange with the –NH₃⁺ protons of the carbamate ion. In the absence of obvious spectral features corresponding to carbamate species in **Fig. 3-2** however, we conclude that carbamic acid (i.e. CH₃CH₂OCH₂CH₂NHCOOH) is the dominant product of EEA-CO₂ complexation in DMSO containing 50 mM EEA at room temperature. This finding is later confirmed via ¹³C NMR and is in good qualitative agreement with what has been

previously reported in literature.¹² It is worth noting that even in a *polar* organic solvent like DMSO, the formation of neutral carbamic acid species is favored over that of charged carbamate species. This seemingly unexpected preferential stabilization of carbamic acid in DMSO is a result of the hydrogen bonding between the sulfonyl group of DMSO and the carboxyl group of the carbamic acid (**Fig. 3-1**).¹²

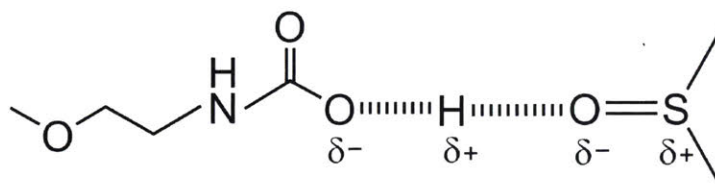


Figure 3-1: Hydrogen-bonded interactions between $-\text{CO}_2\text{H}$ group of the carbamic acid and $\text{S}=\text{O}$ group of DMSO.¹²

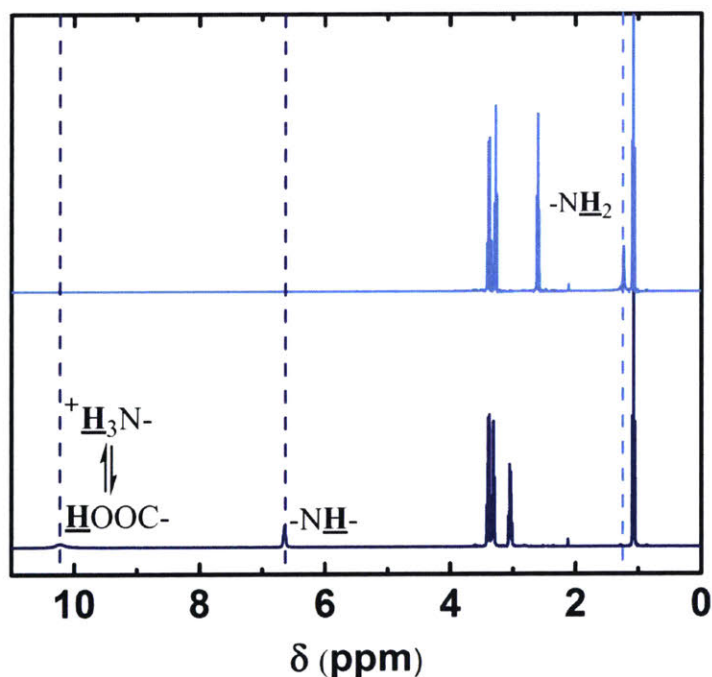


Figure 3-2: ^1H NMR spectra of 50 mM lean EEA (top) and loaded EEA (bottom) in DMSO-d_6 .

The reaction mechanism between amine EEA and CO₂ in DMSO is shown in **Fig. 3-3** and can be described as follows¹²: lean EEA binds the free CO₂ to form an unstable zwitterion, which can undergo an intramolecular proton transfer to form carbamic acid species. Carbamate species on the other hand are formed via deprotonation of either the zwitterion or the carbamic acid species by a lean amine.

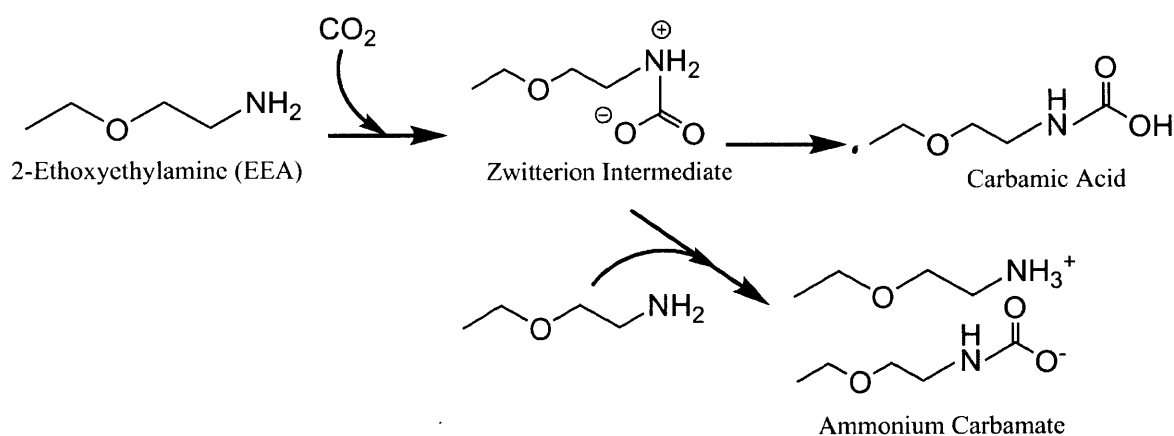


Figure 3-3: Mechanism of carbamate and carbamic acid formation from the chemical absorption of CO₂ by the primary amine EEA via a zwitterion intermediate in DMSO-d₆.

Upon the addition of 0.3 M LiClO₄ in a solution composed of 0.1 M EEA in DMSO, the carbamate salt is hypothesized to undergo a double displacement reaction with LiClO₄ to form lithium carbamate and ammonium perchlorate (**Fig. 3-4**), one or both of which are precipitated out of solution. Note that the reaction between carbamic acid and lithium perchlorate to form perchloric acid and lithium carbamate (RNHCOOH + LiClO₄ → RNHCOOLi + HClO₄) cannot spontaneously occur because it requires the formation of strong acid (HClO₄) from a weak acid (RNHCOOH) for which the Gibbs free energy change is positive ($\Delta G_r > 0$).

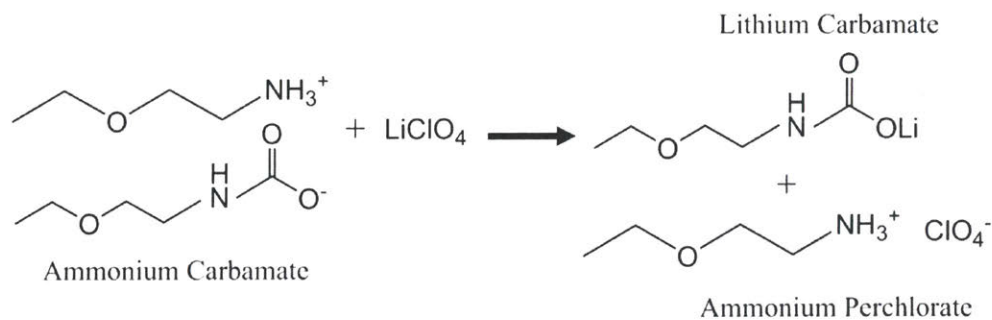


Figure 3-4: Reaction between ammonium carbamate and lithium perchlorate to form ammonium perchlorate and lithium carbamate.

As the ammonium carbamate salt is converted upon reaction with LiClO_4 , it is depleted in solution, which shifts the equilibrium between carbamic acid and carbamate salt towards greater carbamate formation. The ammonium carbamate in solution then further reacts with LiClO_4 , as shown in the reaction above, which helps to explain the increase in observed precipitate over time. **Figure 3-5** depicts a scenario that accentuates this precipitation effect in the electrolyte by utilizing electrolyte samples containing relatively high amine and salt concentrations.

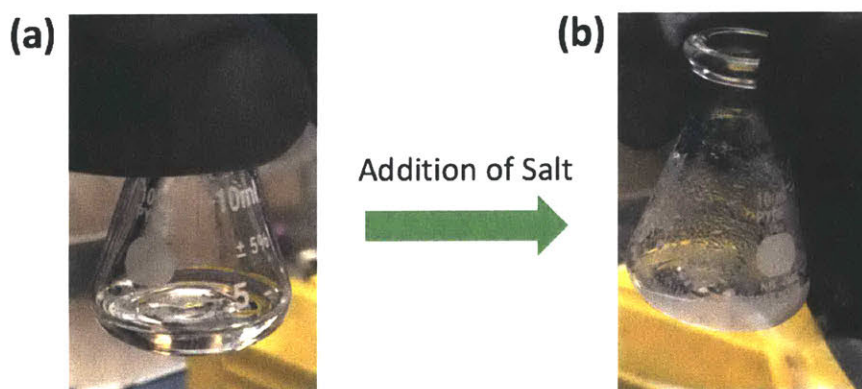


Figure 3-5: Photographs showing 0.5 mL of (a) pure DMSO with 2 M CO_2 bound EEA and (b) 2 M LiClO_4 in DMSO with 2 M CO_2 -bound EEA.

Moreover, our experimental investigations revealed that the electrolyte composed of 0.1 M loaded EEA in 0.3 M LiClO₄ in DMSO was only able to retain the complexed EEA species in solution up to a certain point in time (several days) after which excessive precipitation made complexed amine species inaccessible for electrochemical reduction. The relatively short “lifetime” of the electrolyte as a result of precipitation in this case necessitated the need for making fresh electrolyte considerably more frequently and is currently one of the greatest challenges of this system.

3.2 Electrochemical Testing of Li-CO₂ Cells with Amine Additives

3.2.1 *Reduction of Complexed Amine Species in a non-aqueous Li-CO₂ cell*

Galvanostatic discharge measurements on Li - CO₂ cells were performed using Swagelok-type cells over a range of current densities from open circuit to a cutoff potential of 2 V vs. Li at room temperature (**Fig 3-6**). As shown in from **Fig. 3-6**, Li-CO₂ cells containing the amine yielded a discharge capacity and fairly steady discharge potential as high as ~2100 mAh/g_{carbon} and 2.9 V respectively, at the lowest applied current density of 10 mA/g_{carbon}. The corresponding gravimetric energy density and gravimetric power at 10 mA/g_{carbon} was ~ 6000 Wh/kg_{carbon} and ~ 29 W/kg_{carbon} respectively. A comparison of a Li-CO₂ cell discharged without the amine additive in the electrolyte at 10 mA/g_{carbon} and 20 mA/g_{carbon} (**Fig. 3-7**) and a Li cell containing lean amine discharged under Argon (**Fig. 3-8**) exhibited negligible capacity, thereby confirming that the obtained discharge potential and capacity in **Fig. 3-6** is attributable to the electrochemical reduction of *complexed* amine species present within the electrolyte.

The decrease in discharge plateau potential observed upon an increase in current density is likely a result of the larger kinetic barriers encountered at higher discharge currents.

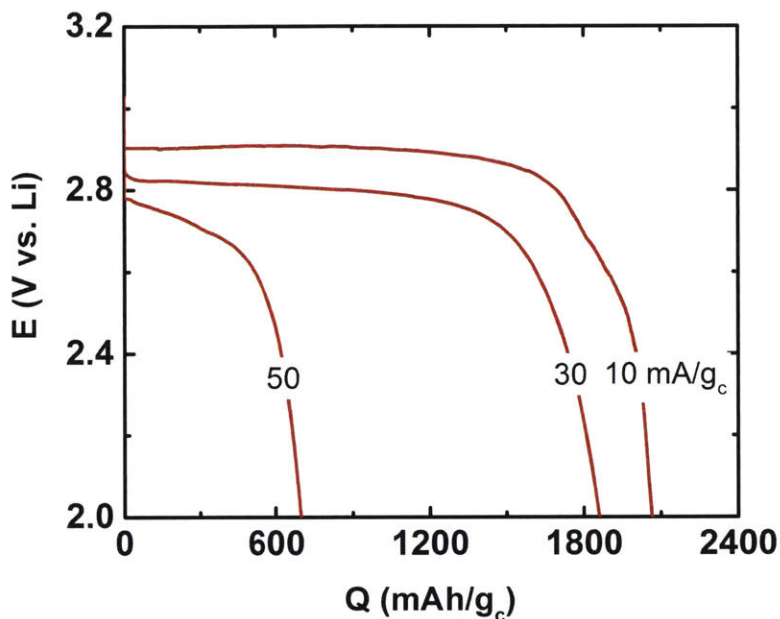


Figure 3-6: Galvanostatic discharge profiles at varying current densities. The electrolyte used was 0.1 M EEA in 0.3M LiClO₄/DMSO.

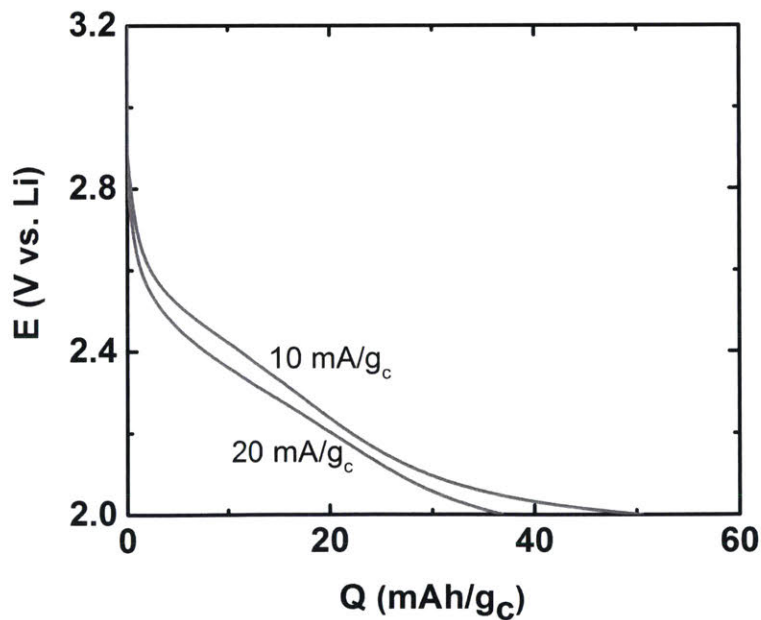


Figure 3-7: Galvanostatic discharge under a pure CO₂ headspace without the addition of amine. The electrolyte used was 0.3 M LiClO₄/DMSO.

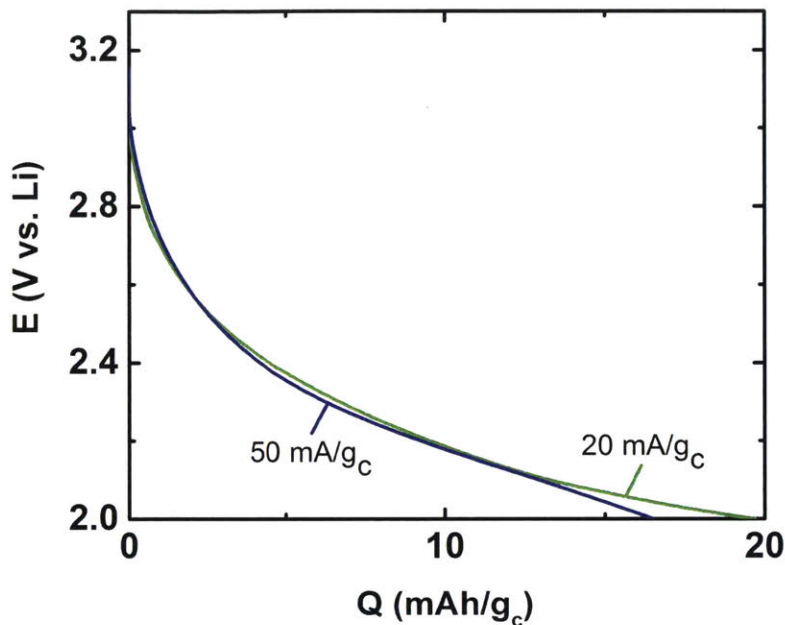


Figure 3-8: Galvanostatic discharge under a pure CO₂ headspace without the addition of amine. The electrolyte used was 0.3 M LiClO₄/DMSO.

3.2.2 Effect of Amine Concentration on Discharge Capacity

To further confirm that the amine could be implicated in the observed high discharge capacities, the effect of amine concentration was also studied under galvanostatic conditions at a fixed current density of 30 mA/g_{carbon} as shown in **Fig. 3-9**. Our results indicated that increasing the amine concentration from 50 mM to up to 115 mM increased the discharge capacity from ~1300 mAh/g_{carbon} to ~2000 mAh/g_{carbon}; however, a further increase in amine concentration to 125 mM resulted in a noticeable decrease in discharge capacity to ~1550 mAh/g and a reduction in discharge plateau potential to a value < 2.8 V (**Fig. 3-10**). This non-monotonic relationship between amine concentration and cell discharge capacity can be explained by considering (a) an increase in the number of electrochemically active loaded amine species at lower concentrations up to the empirically optimized value of 115 mM and (b) thereafter, an increase in solution viscosity observed upon EEA-CO₂ complexation at

higher concentrations. In the region where amine concentration is positively correlated to discharge capacity, i.e. from 50 mM to 115mM, (a) is the dominant effect. However, when amine concentration is pushed past 115 mM to 125 mM, (b) becomes the dominant effect. In this region, the higher solution viscosity imposes transport limitations on the system, thereby adversely affecting the discharge capacity and discharge potential of the Li-CO₂ cell.

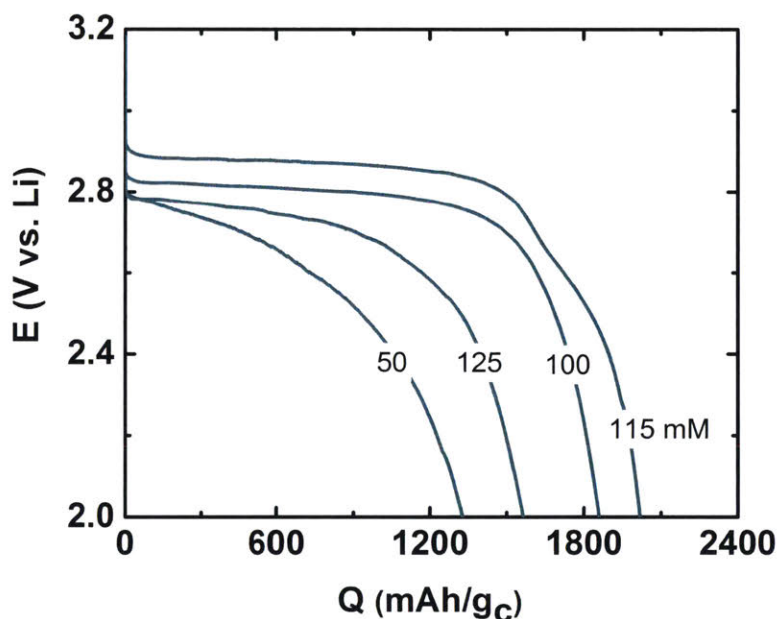


Figure 3-9: Galvanostatic discharge at 30 mA/g at varying amine concentrations. The electrolyte used was 0.3 M LiClO₄ in DMSO.

Overall, the galvanostatic discharge data presented in this section strongly suggests that energetics of the CO₂ molecule can be tailored by chemically complexing CO₂ with a suitable binding agent. Recall that in the absence of any stabilization of the reaction intermediate (CO₂⁻), or a CO₂ “pre-activation” step such as the one proposed herein, a linear CO₂ molecule is always first converted to a bent CO₂ anion radical upon reduction, which typically proceeds at fairly low potentials (-1.9 V vs SHE or ~1.1 V vs. Li). Our results however indicate that by bending

the CO₂ molecule prior to electrochemical reduction through use of a molecular CO₂ sorbent such as an amine, we completely avoid intermediacy of the CO₂ anion radical intermediate formation and are consequently able to reduce bound CO₂ to solid phases at significantly higher potentials (~ 2.7-2.9 V vs. Li).

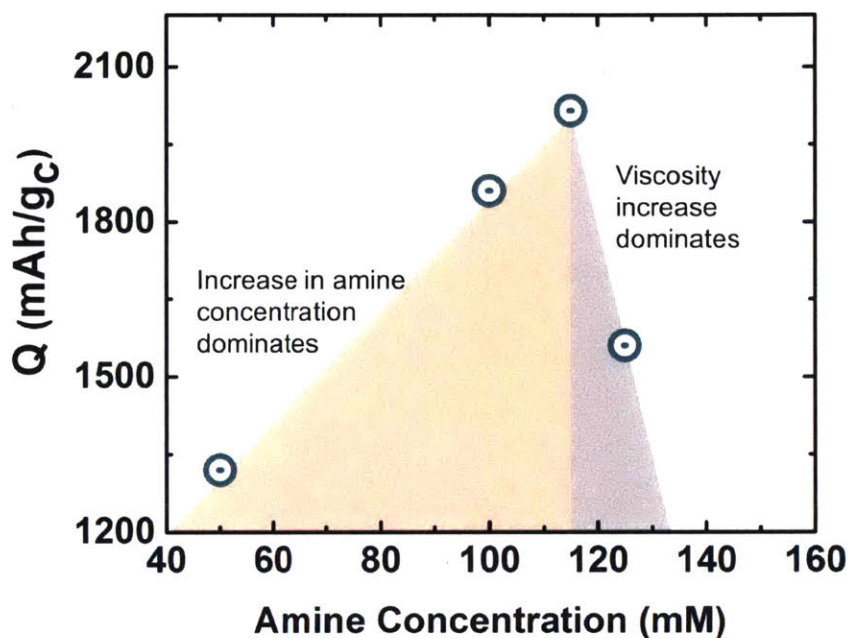


Figure 3-10: Plot of discharge capacity vs. amine concentration indicating an optimal amine concentration.

3.3 Solid-Phase Discharge Product Characterization

The composition of post-discharged electrodes was determined ex situ via infrared (IR) analysis and scanning electron microscopy (SEM). **Fig. 3-11** shows the infrared spectrum of a Vulcan carbon cathode after a galvanostatic discharge at 30 mA/g_{carbon} with 0.1 M EEA (red curve). Upon comparison with an electrode discharged without amine (orange curve), the electrode discharged in the presence of amine exhibits several additional noticeable peaks. The strong transmittance peaks at 1426 cm⁻¹ and 864 cm⁻¹ are characteristic of the antisymmetric stretch and out-of-plane bending mode of amorphous carbonate ion,^{62,63} indicating that

amorphous lithium carbonate is the predominant solid-phase discharge products formed upon the electrochemical reduction of complexed amine species in the Li-CO₂ battery. The lack of N-H and N-C stretches in the IR spectrum of the solid-phase discharge product, which typically appear between the ranges 3300-3500 cm⁻¹ and 1080-1360 cm⁻¹ respectively, indicates that the amine or derived products were not incorporated in the solid phase, which suggests that electrochemical reduction selectively cleaves the -N-C- bond to liberate reduced CO₂ products - a finding that is later confirmed via ¹³C NMR in **Fig. 3-17**. The amorphous nature of the carbonate formed upon discharge is also consistent with XRD spectrum of our discharged cathode, which indicates the absence of any crystalline, solid-phase products (**Fig. 3-12**).

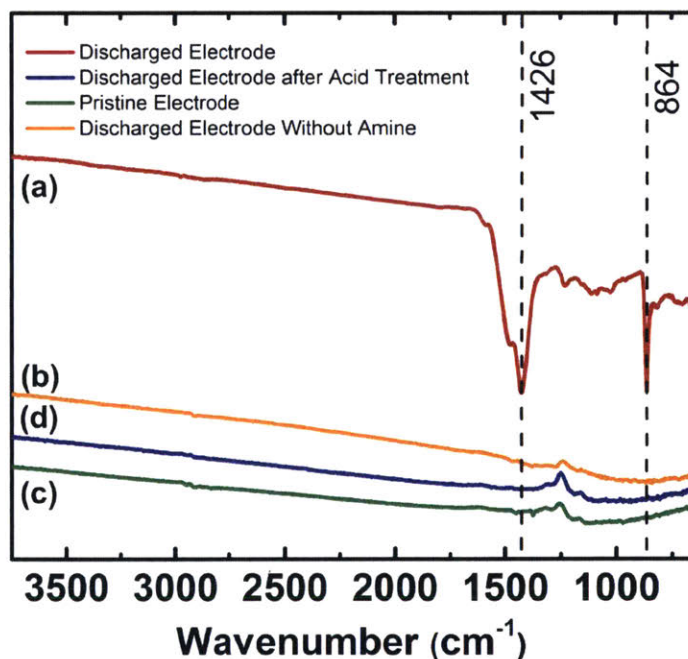


Figure 3-11: Infrared spectra of (a) carbon cathode after a galvanostatic discharge at 30 mA/g_{carbon} with 0.1 M EEA; (b) carbon cathode after a galvanostatic discharge at 30 mA/g_{carbon} with no amine; (c) a pristine cathode; and (d) the electrode from (a) after treatment with 2 M H₃PO₄.

To further confirm the presence of amorphous lithium carbonate, the discharged cathode was soaked in 2 M phosphoric acid (H₃PO₄) for several hours and an infrared spectrum

was subsequently remeasured. The blue curve in **Fig. 3-11**, which shows the IR spectrum of the discharged cathode post treatment with acid, does not exhibit any of the characteristic IR peaks of amorphous lithium carbonate; in fact, it closely resembles the pristine cathode (green curve). This suggests that in line with our expectations, the lithium carbonate formed upon discharge completely reacted away upon exposure to phosphoric acid to evolve CO₂.

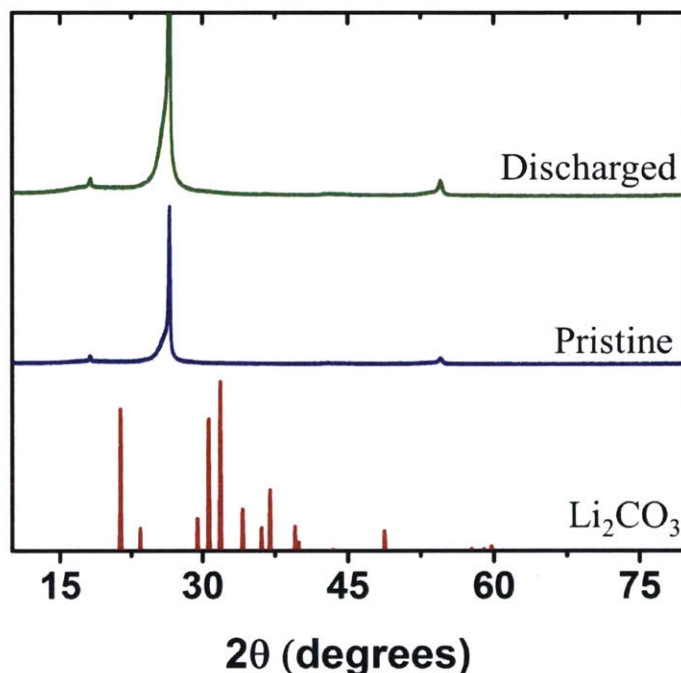


Figure 3-12: X-Ray diffraction scans of a pristine and a galvanostatically discharged Toray paper electrode. The applied current density was 30 mA/g and the electrolyte used was 0.1 M EEA in 0.3 M LiClO₄ in DMSO. The XRD spectrum of crystalline lithium carbonate is provided as a reference.

To investigate the formation and morphology of solid-phase discharge products, SEM imaging was conducted on the discharged electrode (**Figure 3-13**). As shown in **Fig. 3-13 (b)**, the electrochemically produced lithium carbonate assumed the shape of small spherical particles with a characteristic length scale of ~ 500 nm that grew within the carbon electrode. As a comparison, an SEM image of Vulcan XC – 72R carbon black, i.e. the pristine cathode, with a measured particle size of around 50 nm, is also provided in **Fig. 3-13 (a)**. The observed

spherical structure of the discharge product is in good agreement with the spherical shape of carbonates.⁶⁴ Furthermore, the uniform distribution of the discharge product coupled with the preserved porous structure of the pristine electrode is indicative of intimate contact and growth of amorphous Li_2CO_3 on carbon. Moreover, the abundance of solid product formed upon discharge, as evident from the SEM images, is not only consistent with the high discharge capacities obtained but is also suggestive of the carbon electrode's ability to accumulate discharge products. A drawback of such solid-phase accumulation on the cathode however is that the electronically insulating Li_2CO_3 formed upon discharge eventually passivates the entire electrode surface, and therefore could contribute for premature termination of discharge.

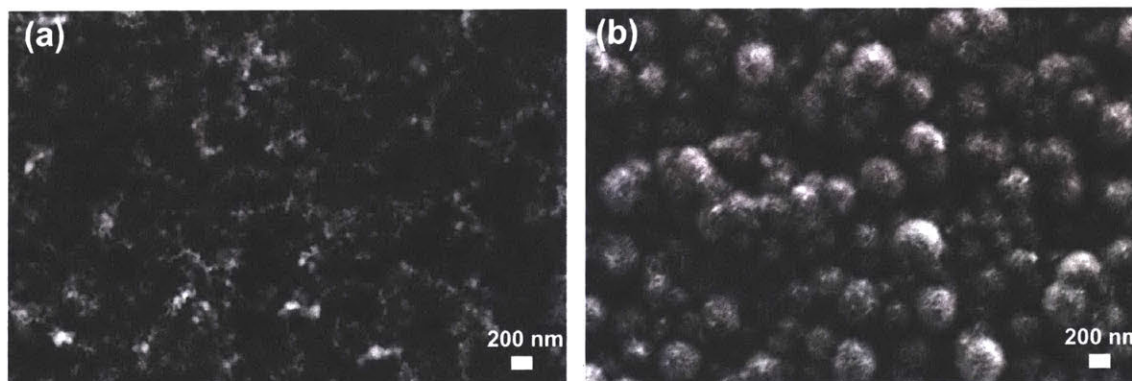


Figure 3-13: SEM images of (a) pristine cathode and (b) discharged cathode (Vulcan Carbon) at 30 mA/g. The electrolyte used was 100 mM EEA in 0.3 M LiClO_4 in DMSO.

To verify that the 3D spherical structure of the electrochemically formed lithium carbonate (as observed in Fig. 3-11) was not a consequence of growth on a spherical substrate such as Vulcan carbon particles, SEM images were also performed on galvanostatically discharged Gas Diffusion Layer (GDL) positive electrodes (**Fig. 3-14**), which enabled the growth of the solid-phase discharge product on planar carbon fibers instead of on spherical carbon particles. As shown in **Fig. 3-14**, electrochemically formed lithium carbonate retains

its spherical shape even on GDL electrodes, thereby confirming the 3-D structure of the discharge product. The characteristic length of the spherical particles observed in this case is measured to be around ~ 500 nm, which is consistent with that observed for discharge product on Vulcan carbon cathodes. A corresponding IR spectra of the pristine and discharged GDL electrodes imaged in **Fig. 3-14** is shown in **Fig 3-15**, which confirms that the product observed in the SEM images is indeed amorphous lithium carbonate.

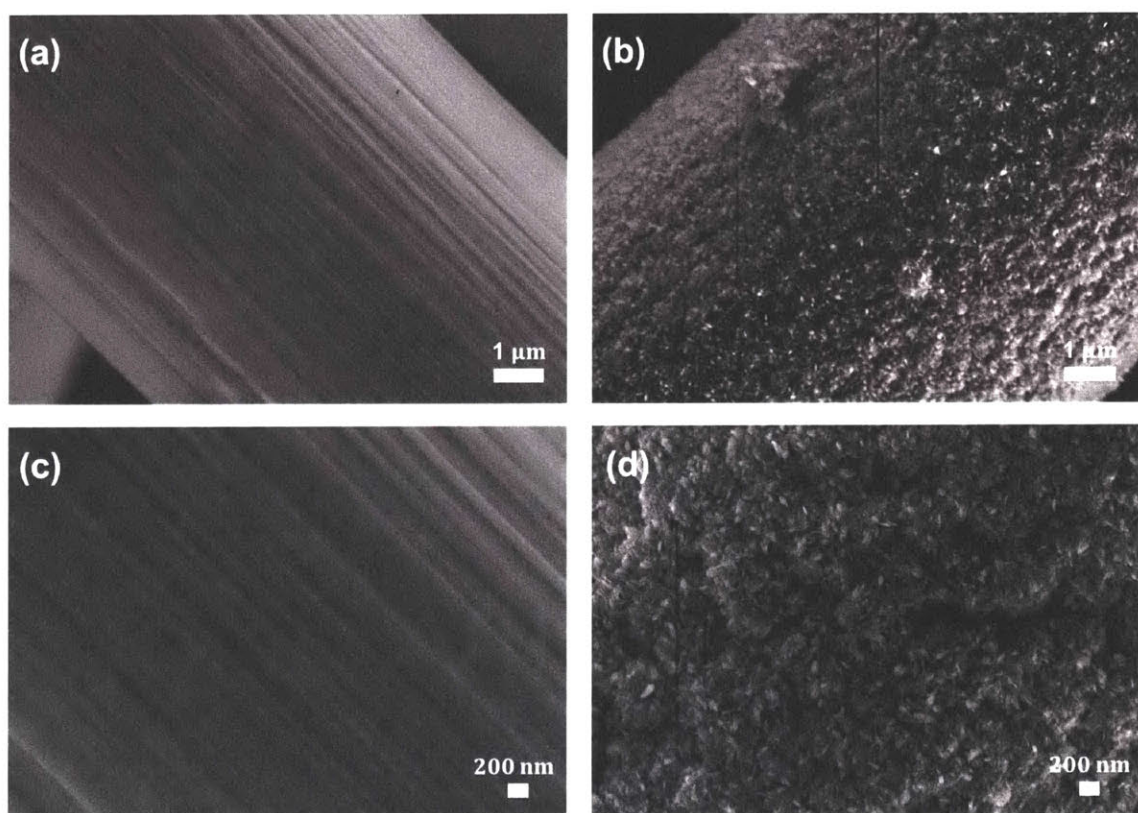


Figure 3-14: SEM images of (a) pristine cathode and (b) discharged cathode (GDL) at 30 mA/g. The electrolyte used was 100 mM EEA in 0.3 M LiClO₄ in DMSO. The top and bottom row images have a corresponding magnification of 10Kx and 20Kx respectively.

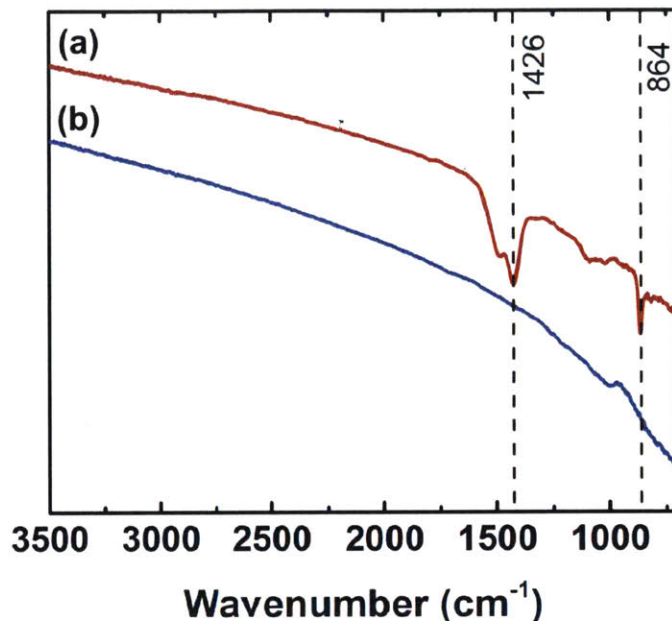


Figure 3-15: Infrared spectra of (a) GDL electrode after a galvanostatic discharge at 30 mA/g_{carbon} with 0.1 M EEA and (b) pristine GDL electrode.

3.4 Detection of Potential Secondary Products

In addition to Li₂CO₃, our system was further tested for secondary discharge product(s) whose identification is necessary to elucidate the complete reaction occurring in our cell. Typically, electrochemical reduction of CO₂ in non-aqueous electrolytes yield either CO or carbon in addition to Li₂CO₃ upon discharge. If CO is being formed alongside Li₂CO₃ (Li + CO₂ → Li₂CO₃ + CO, E⁰ = 2.49 V vs. Li), then the stoichiometry of the reaction dictates that the molar ratio of Li₂CO₃ to CO be 1:1. To check for CO formation in our system, both CO and lithium carbonate were quantified using GC analysis of headspace gas and ⁷Li NMR respectively. **Fig 3-16 (a)** shows the galvanostatic discharge curves of two cells at different current densities for which quantification experiments were conducted. **Fig 3-16 (b)** shows the corresponding ⁷Li NMR spectra obtained for quantifying amount of lithium carbonate electrochemically formed upon discharge. Li₂CO₃ and CO quantification results corresponding to each of the two cells are tabulated in **Table 3-2**.

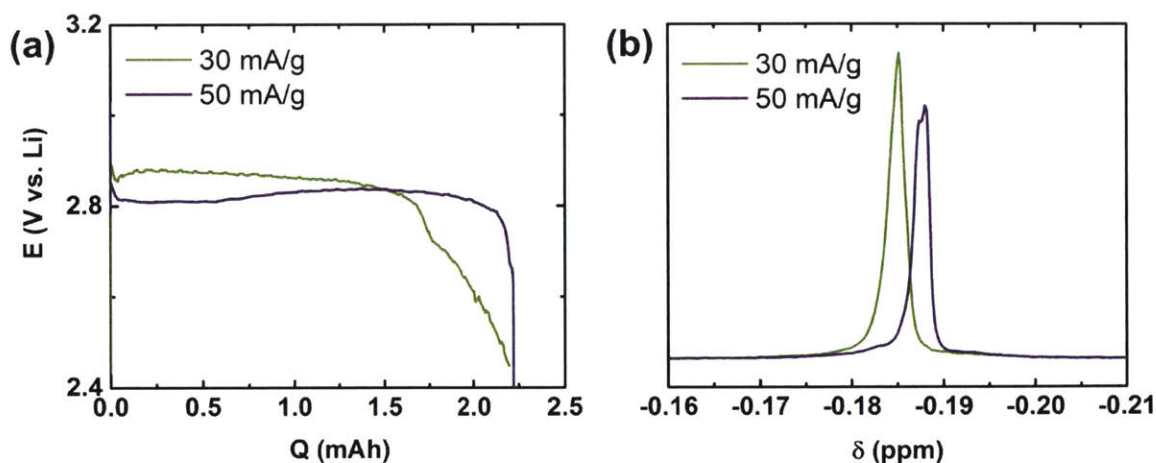


Figure 3-16: Galvanostatic discharge on GDL electrodes at varying current densities (a) and the corresponding ^7Li NMR spectra obtained for Li_2CO_3 quantification. The electrolyte used was 0.1 M EEA in 0.3 M LiClO_4 in DMSO.

I (mA/g)	Li_2CO_3 (mol)	CO (mol)	η_{Faradaic} (%)
30	1.72×10^{-5}	9.5×10^{-8}	41.9
50	1.35×10^{-5}	9.8×10^{-8}	32.5

Table 3-2: Lithium carbonate and carbon monoxide quantification results obtained for the cells shown in Fig. 3-14 (a).

As shown in the **Table 3-2**, for both the 30 and 50 mA/g cases, the moles of CO in the headspace post discharge are close to two orders of magnitude lower than the moles of lithium carbonate formed on the cathode, which indicates that carbon monoxide is not a major discharge product in our cell. It is worth noting that the low Faradaic efficiency obtained for carbonate formation in both cases may be a result of the loss of discharge product incurred upon rinsing the discharged cathode with DME prior to sample preparation for ^7Li NMR. Though undesirable, the cathode rinse step is necessary for quantifying lithium carbonate using ^7Li NMR to ensure that the electrolyte salt (LiClO_4), which also contains solvated Li ions, is completely washed away. Alternative quantification techniques such as titration or differential

electrochemical mass spectrometry (DEMS) that eliminate the need for cathode rinses prior to carbonate quantification may be needed to more accurately determine the Faradaic efficiency of our system.

In the absence of carbon monoxide, carbon may be a likely secondary product alongside lithium carbonate ($4\text{Li} + 3\text{CO}_2 \rightarrow 2\text{Li}_2\text{CO}_3 + \text{C}$, $E^0 = 2.8 \text{ V vs. Li}$) in our cells. However, as of yet, we do not have any evidence for carbon formation largely because carbon detection in a system like ours, where the reduction process is most typically carried on a carbon electrode, is challenging. Possible carbon formation on the discharged positive electrode in the proposed system is currently under investigation.

It is imperative to note that both candidate reactions - $4\text{Li} + 3\text{CO}_2 \rightarrow 2\text{Li}_2\text{CO}_3 + \text{C}$ and $\text{Li} + \text{CO}_2 \rightarrow \text{Li}_2\text{CO}_3 + \text{CO}$ - mentioned above have thermodynamic equilibrium potentials (E^0) that are *higher* than the experimentally observed potential ($\sim 2.9 \text{ V vs. Li}$) at the lowest applied current density (10 mA/g_c) in our system. This not only suggests that the full cell reaction occurring in our system is likely different from the aforementioned reactions, but also indicates that Gibbs free energy change ($\Delta G_r = -nFE^0$) of the full cell reaction occurring in our system, which uniquely employs an amine for the CO_2 pre-activation step, is larger (more negative) than that for the aforementioned reactions.

3.5 Fate of the Amine upon Electrochemical Reduction of Complexed Amine Species

In order to examine the fate of the amine during the electrochemical reduction of complexed amine species, ^{13}C NMR measurements were performed on the electrolyte (a) prior to reduction, (b) post electrochemical reduction and (c) following a CO_2 purge after reduction. For this study, electrochemical measurements were conducted using a 3-electrode electrolysis-

type cell containing a Li metal counter electrode, a nonaqueous AgNO₃ reference electrode, and a carbon cloth (1071 HCB, Fuel Cell Store) working electrode. The electrolyte solution containing 50 mM EEA in 0.3 M LiClO₄ in DMSO was purged with carbon-13 dioxide (99 atom % ¹³C, Sigma Aldrich) for 20 seconds prior to cell assembly. Once the cell was assembled, a small sample volume (600 μL) was drawn for ¹³C NMR analysis. **Figure 3-17 (a)** shows the ¹³C NMR spectrum of this initial sample. The ¹³C NMR resonance corresponding to NH-COOH – and NH-COO⁻ equilibrium mixture is observed at 158.2 ppm, indicating that carbamic acid is the dominant product of EEA-CO₂ complexation in the given electrolyte, consistent with earlier results from ¹H NMR. The resonance peak at 125.1 ppm is associated with the physical absorption of CO₂ in the electrolyte.

To determine whether or not the N-C bond is cleaved upon electrochemical reduction of complexed amine species (indicative of selective reduction of the bound CO₂), cyclic voltammetry experiments were performed at 50 mV/s from 3 V vs. Li to 1 V vs. Li for 600 cycles. A magnetic stir bar was used to thoroughly mix the electrolyte to improve reaction kinetics and to ensure all complexed amine species were reduced. The ¹³C NMR spectrum of a sample drawn after all complexed amines had visibly cycled away (i.e. when the observed reduction current was negligible indicated a cleavage of N-C- bond upon electrochemical reduction, as evidenced by the absence of NH-C- resonance peak shown in **Fig. 3-17 (b)**). Upon re-purging the electrolyte with ¹³CO₂ post electrochemical reduction for 20 seconds and re-performing ¹³C NMR analysis, we found no further chemical absorption of CO₂ by the electrolyte, even though some CO₂ was physically absorbed (**Fig. 3-17 (c)**). The inability of the amine additive to rebind with CO₂ after the post-reduction purge reveals that the amines are not regenerated and are likely irreversibly altered during the course of reduction.

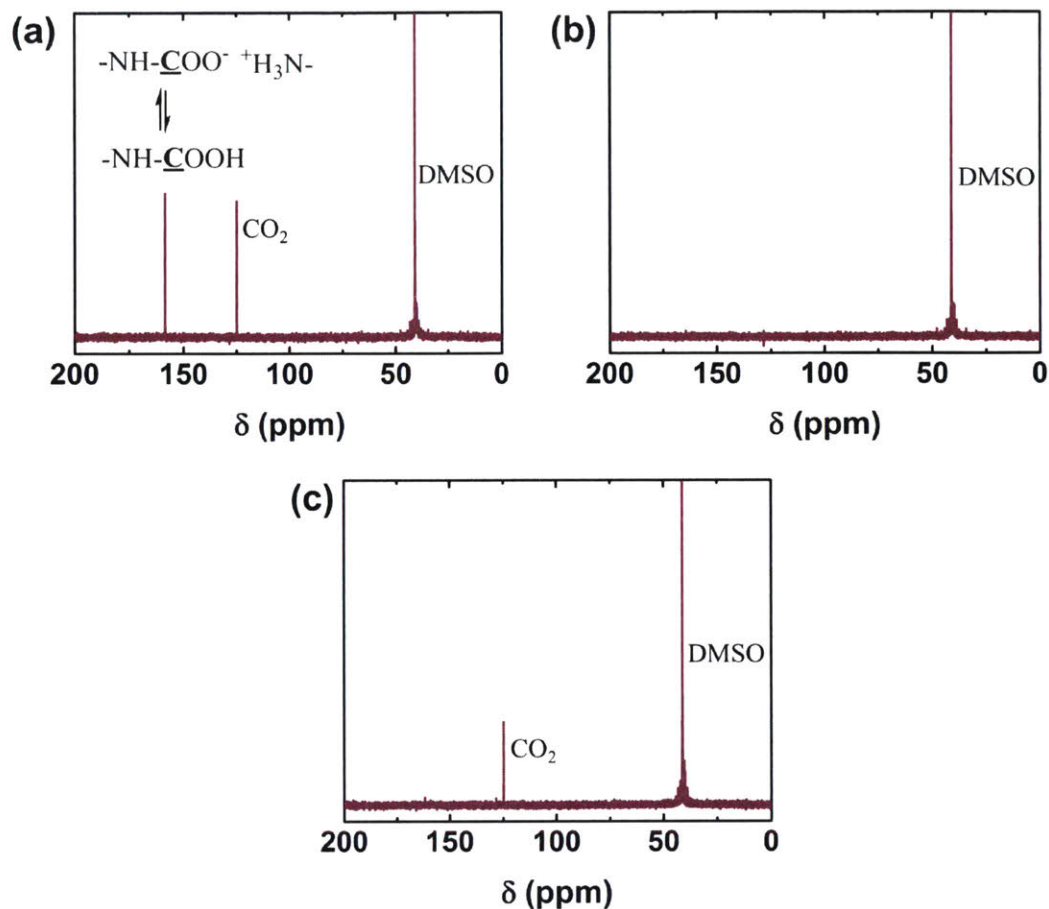


Figure 3-17: ^{13}C NMR spectrum of 50 mM EEA in 0.3M LiClO_4 in DMSO prior to reduction (a), post electrochemical reduction (b), and CO_2 purge after reduction (c).

To further confirm this finding, ^1H NMR was also performed on the electrolyte (0.1 M EEA in 0.3 M LiClO_4 in DMSO-d_6) in a Swagelok cell before and after discharge (**Fig. 3-18**). As shown in **Fig. 3-18**, ^1H NMR spectrum of the electrolyte post discharge indicated an absence of the $-\text{NH}_2$ resonance at ~ 1.3 ppm which characteristic of a lean, or successfully regenerated amine. Overall, while there are some obvious changes in the ^1H NMR spectrum of amine before and after discharge which may adequately explain amine inactivation, the complexity of the system makes it extremely difficult to conclude what exactly remains of the amine post electrochemical reduction from the NMR spectra shown in Fig. 3-18 alone. At this

point, additional experimental and computational tools are needed to not only needed to correctly interpret the NMR data provided but also explore alternative avenues to a reach definitive conclusion regarding the final state of the amine.

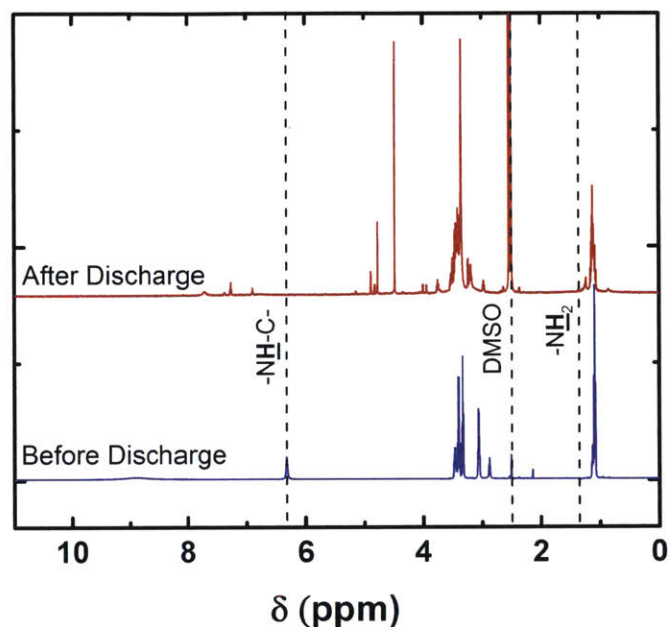


Figure 3-18: ^1H NMR spectrum of 50 mM EEA in 0.3M LiClO_4 in DMSO- d_6 (not deuterated) following electrochemical reduction.

3.6 Cyclic Voltammetry Studies on the Reduction of Loaded Amine Species

The electrochemical reduction of loaded amine species was also studied using cyclic voltammetry in a 3-electrode electrolysis type cell using a glassy carbon (GC) working electrode, a platinum wire counter electrode, and a nonaqueous AgNO_3 reference electrode (Ag wire immersed in 0.1 M TBAClO_4 / 0.01 M AgNO_3 in acetonitrile, calibrated against a Li metal electrode in 3 mL of 0.3 M LiClO_4 in DMSO (0 V vs. $\text{Li/Li}^+ = -3.700\text{V}$ vs. Ag/Ag^+)). **Fig. 3-19** shows a comparison of the reduction of chemically complexed CO_2 (loaded amine species) and physically dissolved CO_2 (no amine). As shown in **Fig. 3-19**, relatively large

reduction currents are obtained upon the electrochemical reduction of loaded amine species whereas no significant activity is observed for uncomplexed CO₂ over the potential window investigated, which is consistent with our results from galvanostatically discharged Li-CO₂ cells.

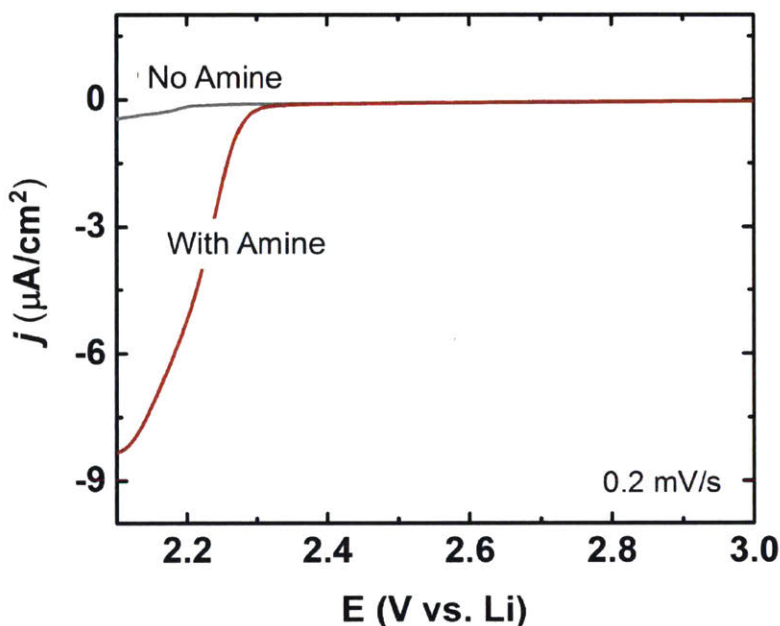


Figure 3-19: Reduction of loaded amine species on glassy carbon at 0.2 mV/s. The electrolyte used was 50 mM EEA in 0.3 M LiClO₄ in DMSO.

The effect of rotation rate on the kinetics of the reduction reaction of loaded amine species was also studied using a rotating disc (GC) electrode (RDE). **Figure 3-20**, which shows current density as a function of the working electrode's potential at three different rotation rates (0 RPM, 900 RPM and 1600 RPM) indicates that increasing the rotation rate improves the reaction kinetics as evidenced by the lower kinetic overpotentials obtained at higher rotation speeds. Furthermore, the magnitude of the reduction current clearly increases with increasing rotation rate which can be attributed to the enhanced convective flux of reactant

species on the electrode surface. It is also worth noting that even for rotation rates as high as 1600 RPM, limiting currents could not be reached which is indicative of surface passivation of the GC electrode surface potentially as a result of a solid-phase formation upon the electrochemical reduction of loaded amine species.

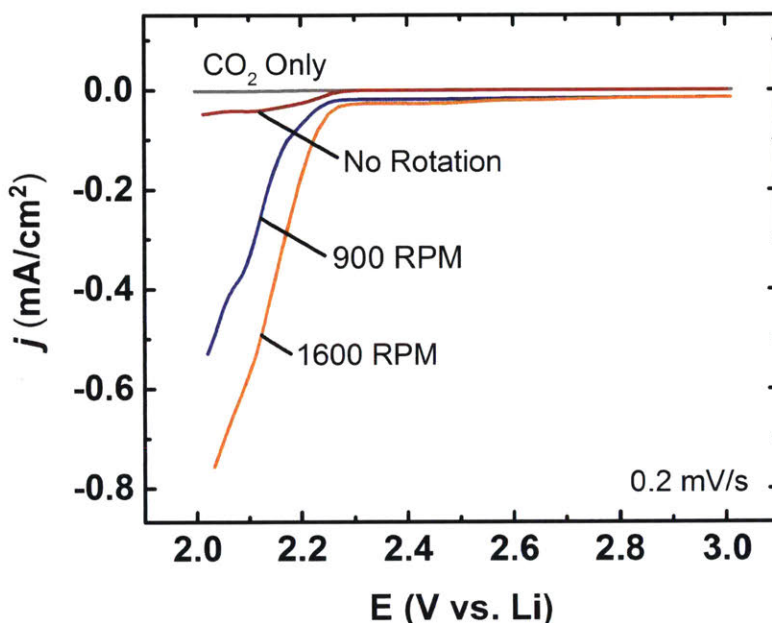


Figure 3-20: Reduction of loaded amine species on glassy carbon at 0.2 mV/s at varying rotation rates. The electrolyte used was 50 mM EEA in 0.3 M LiClO₄ in DMSO.

3.7 Experimental Determination of the Maximum Achievable Potential

To determine the maximum achievable discharge potential in our system, potentiodynamic cycling with galvanostatic acceleration (PCGA), a technique very similar to the potentiostatic intermittent titration technique (PITT),⁶⁵ was performed on our Li-CO₂ cell. Typically, PCGA is used to determine the minimum overpotential to drive an electrochemical reaction in a system where the thermodynamic potential is known. However, in a system like ours where the thermodynamic potential is difficult to measure directly,

PCGA merely provides an estimate for the maximum achievable discharge potential. The results from the PCGA discharge are shown in **Fig. 3-21**, indicating ~ 2.96 V as approximately the highest discharge potential attainable in our system.

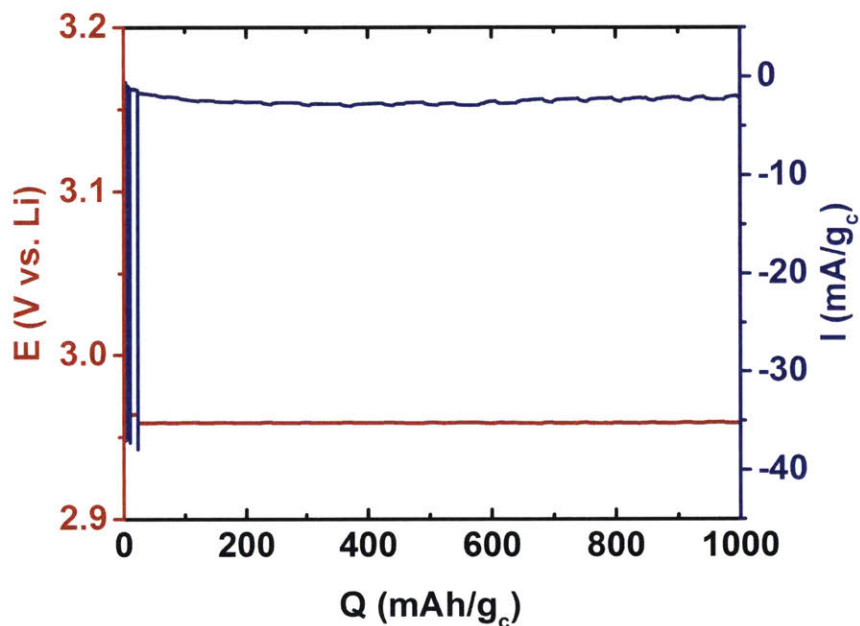


Figure 3-21: Potentiodynamic cycling with galvanostatic acceleration (PCGA) discharge of a Vulcan carbon electrode from open circuit (~ 3.05 V vs. Li). The potential step amplitude was 5 mV and the current cutoff per step was 0.5 mA/g_c .

4 ADVANTAGES OF AMINE-MEDIATED NON-AQUEOUS CO₂ REDUCTION

The amine-mediated electrochemical CO₂ reduction in a non-aqueous electrolyte proposed herein offers several advantages over conventional capture based technologies and classical CO₂ reduction. To evaluate the advantages of the proposed combined chemical-electrochemical CO₂ capture and conversion approach, it is useful to compare it to the existing CO₂ management technologies broadly encompassing both chemical capture and electrochemical conversion.

Advantages compared to CO₂ capture

The main technological and economic hurdles associated with conventional amine capture technologies are: (1) The energy intensiveness of the CO₂ regeneration step at moderate temperatures (~40 °C) is approximately ~80 kJ/mol,¹⁴ achieved *via* thermal or pressure-swing desorption and requiring up to 30% of the plant's power output to drive the reaction at scale;¹⁶ (2) Energy losses due to the latent heat of vaporization of water, an undesirable yet unavoidable parallel process in aqueous-based systems; (3) Thermal degradation of costly amines⁶⁶; and (4) Additional energetic and logistical costs associated with compression, transport and (untested) long-term geological storage of liquefied CO₂.¹⁴ CO₂ sequestration not only requires compression of CO₂ at high pressures which is costly, but also poses a risk of atmospheric or subsurface leakage of CO₂ from storage sites which can have detrimental effects on human health and the environment. Efforts to address (1) – (2) have mainly focused on tailoring the amine chemistry for improved CO₂ release energetics, but improvements have been incremental.

An alternative to the conventional temperature and pressure-swing CO₂ desorption processes is the EMAR process, in which the amine is regenerated by an electrochemically driven process rather than thermally as mentioned earlier. The EMAR process for amine regeneration is more energetically efficient compared to thermal regeneration as a result of the ability of electrochemical processes to selectively attack target molecules instead of the entirety of the medium. EMAR systems can also desorb CO₂ at higher pressures and therefore can significantly reduce the costs associated with CO₂ compression required prior to storage.² Despite its several advantages over conventional CO₂ capture technologies however, the EMAR cycle still remains an electrolytic process requiring an energy input for operation much like traditional scrubbing technologies.

The reported system presents a potential competitive advantage over existing systems by using reducing electrons, rather than high temperatures, to effect the CO₂ reduction. Therefore, it accomplishes CO₂ capture and reduction at room temperatures. This intrinsically obviates the critical issues (1) - (2), which together currently limit the adoption of capture technologies. Our process also forms a solid which relieves the dependence on underground storage of compressed CO₂, providing an alternative to (4). If the rebinding of CO₂ can be optimized and parasitic reactions minimized, it may also be possible to address challenge (3) if the deactivation of amines can be adequately addressed. Furthermore, the amine assisted Li-CO₂ reaction presented herein acts as a galvanic cell, which outputs a voltage (~2.77 – 2.9 V vs. Li) and useful electrical work. Therefore, our CO₂ mitigation technology can also successfully harvest energy from the CO₂ molecule and has the added advantage of potentially serving as an energy harvesting device or as a primary battery with high capacity and energy density.

Advantages compared to aqueous CO₂ reduction

Electrochemical methods for CO₂ conversion such as the aqueous electrochemical reduction of CO₂ can theoretically convert CO₂ to a wide variety of energy-rich products.⁴² Practically, however, the kinetic limitations of the process are severe, such that reactions must be driven at high overpotentials (~ 1 V) to obtain significant yields and selectivity.³⁴ Separation and accumulation of products (often a range of reduced carbon products) is particularly challenging, representing a major impediment to viability. Recently, researchers have been exploring the use of so-called “task-specific” ionic liquids to promote favorable energetics of the absorbed CO₂ through complexation with electrolyte anions.^{28,31,45,67} Selectivity for CO has been demonstrated with low overpotentials for the CO₂ reaction, but the aqueous system still requires a balancing O₂ evolution / water electrolysis reaction at the anode side to liberate protons from water, which yields required cell voltages (energy input) of ~1 V or higher. Moreover, the yield for energy-rich fuel products (methane or, e.g., ethylene) has been insignificant to date.

The proposed approach offers several potential advantages over aqueous CO₂ reduction. First, it eliminates the need for the energy intensive water-splitting process, which is the balancing reaction at the anode. Second, our technology has the potential to enable the use of alkali metals like sodium or calcium as the negative electrode materials, which may be more cost effective than the oxygen evolving catalysts commonly employed at the anode in aqueous media. Third, the high overpotentials incurred upon aqueous CO₂ reduction give rise to limited product selectivity and necessitates a need for product separation, while our device converts gas-phase CO₂ into a more tractable, benign solid-phase substance (Li₂CO₃) that conveniently

grows within the electrode, making subsequent recovery and treatment of the solid-phase product potentially easier. Lastly, unlike aqueous media, the large voltage window afforded by the use of nonaqueous electrolytes in our device, coupled with the presence of tunable system parameters like potential and current is particularly beneficial because it allows us to simultaneously probe chemical activity over a large energy range while providing a range of parameters to control reaction pathways.

Advantages compared to nonaqueous CO₂ reduction

Nonaqueous electrochemical reduction of CO₂ in organic battery electrolytes has also been investigated in Li-based CO₂ batteries. However, the large kinetic barriers associated with CO₂ activation have presented significant hurdles such that only limited systems have reported any reduction activity of CO₂ to date. CO₂ has been previously studied as a contaminant in Li-air batteries where CO₂ activation has only been achieved via a chemical reaction with the electrochemically generated oxygen anion radical species.^{45,54} Non-aqueous CO₂ reduction has also been observed in a Li-CO₂ battery employing an ionic liquid electrolyte but only at higher temperatures (60 degrees – 100 degrees).⁴⁴

In contrast, our CO₂ mitigation device uses a combined chemical-electrochemical approach to efficiently drive molecular activation and subsequent conversion of CO₂ at room temperature while harvesting energy in the form of a voltage output. By employing chemisorption to affect bending of the linear CO₂ molecule prior to electrochemical reduction, amines present in the electrolyte help to significantly reduce the prohibitively large kinetic overpotential associated with first electron transfer step responsible for converting the linear CO₂ molecule to the bent CO₂⁻ anion radical.

5 CONCLUSION AND FUTURE WORKS

The central advancement reported through this thesis is the first-time coupling of CO₂ capture chemistry (aqueous-based) to nonaqueous electrochemistry, which allows CO₂ to be reduced with reasonable kinetics at an uncatalyzed electrode and for energy to be concurrently extracted from the conversion reaction owing to the high exothermicity of the reaction with alkali metals. In developing this system, we have adapted aqueous amine chemistry and applied it in a new way. Our proposed Li-CO₂ system utilizes a CO₂ sorbent, namely 2-ethoxyethylamine in a nonaqueous electrolyte (DMSO) to chemically bind the CO₂ prior to electrochemical reduction. The chemisorption step bends the inert, linear CO₂ molecule through the formation of an -N-C- bond, and therefore decouples the first electron transfer step from the structural rearrangement of the CO₂ molecule, which facilitates the rate-limiting step in classical electrochemical CO₂ reduction. Our results indicate that electrochemical reduction of lithium carbamate, which is formed in solution as a result of the reaction between loaded amine species (ammonium carbamate) and LiClO₄, is kinetically accessible and proceeds at considerably higher discharge potentials (~2.9 V vs. Li) compared to that observed in the reduction of purely physically dissolved (uncomplexed) CO₂. Furthermore, galvanostatic testing of our Li-CO₂ cells demonstrated that our cells can yield high discharge capacities (>1000 mAh/g_c) and therefore can be used to achieve CO₂ emissions reductions while offsetting additional energetic costs by effectively serving as primary batteries. The effect of amine concentration in our system was also studied which revealed that both the cell discharge capacity and discharge potential can be boosted by increasing the amine concentration but only up to a certain point (~115 mM) after which further increases in amine concentration begin to adversely affect discharge capacities and potentials as a result of significant viscosity increases

incurred upon increasing amine concentration. Moreover, while the complete full cell reaction occurring in our system is not yet known, solid-phase discharge product characterization techniques have revealed that our Li-CO₂ system converts solution phase loaded amine species into a predominantly, benign solid-phase (lithium carbonate) through selectively cleaving the -N-C- bond upon electrochemical reduction, which is arguably safer and potentially easier from a storage standpoint.

It is also worth noting that our CO₂ capture and conversion technology can operate with readily available, mass market-produced materials at room temperatures and does not require an energy input. Furthermore, our technology harvests electrical energy, in the form of a voltage output, from the flow of a waste gas. Therefore, it has the additional value as self-powered sensing device or energy harvester, which can redirect captured energy back into industrial cycles.

Future work on this project will seek to not only address some of the existing challenges of the system, but also explore new chemistries that could help improve both battery performance and mechanistic understanding of the underlying cell reaction. Firstly, to improve the “lifetime” of the electrolyte, the issue of salt precipitation in the electrolyte needs to be addressed. Recall from before that within the electrolyte, a double displacement reaction between ammonium carbamate and lithium perchlorate produces lithium carbamate and ammonium perchlorate, one or both of which are precipitated out of solution after a certain period of time has elapsed. Future work will (a) seek to precisely identify which one of these two products is responsible for precipitation and (b) identify ways such as tuning the size,

nature, or concentration of electrolyte salt's cation or anion that could help boost the solubility of these species in the electrolyte.

Secondly, in the work done thus far, the end state of the amine still remains unclear. We know that the -N-C bond is cleaved during reduction but reason behind the inactivation of the amine is not yet evident. A thorough understanding of the final state of the amine after cell discharge is instrumental for determining the full cell reaction occurring in our system. Future work will focus on not only identifying what remains of the amine post electrochemical reduction through both experimental and computational means but also investigating what prevents the amine from regaining its proton upon N-C - bond cleavage to regenerate itself. Amine regeneration is an essential component of this work. Ideally, we would like to accomplish a system similar to that shown in **Fig. 5-1** where the amine is regenerated post electrochemical reduction of loaded amine species in the electrolyte and can continue to rebind with CO_2 for form a complete, closed cycle.

Thirdly, it is known that CO_2 complexation with amine can drastically increase the viscosity of the electrolyte, a parameter which plays a key role in determining battery performance. It is known that highly viscous electrolytes significantly increase transport barriers in the cell and can adversely affect discharge potentials and capacities. Future work will therefore also look into how viscosity of CO_2 adducts can be reduced so that the optimal amine concentration and correspondingly the discharge capacity can be boosted further, provided we are not limited by the surface area of the cathode. Eliminating drastic viscosity increases incurred upon CO_2 complexation will also make the use of greener, and more stable solvents like ionic liquids for the proposed system possible.

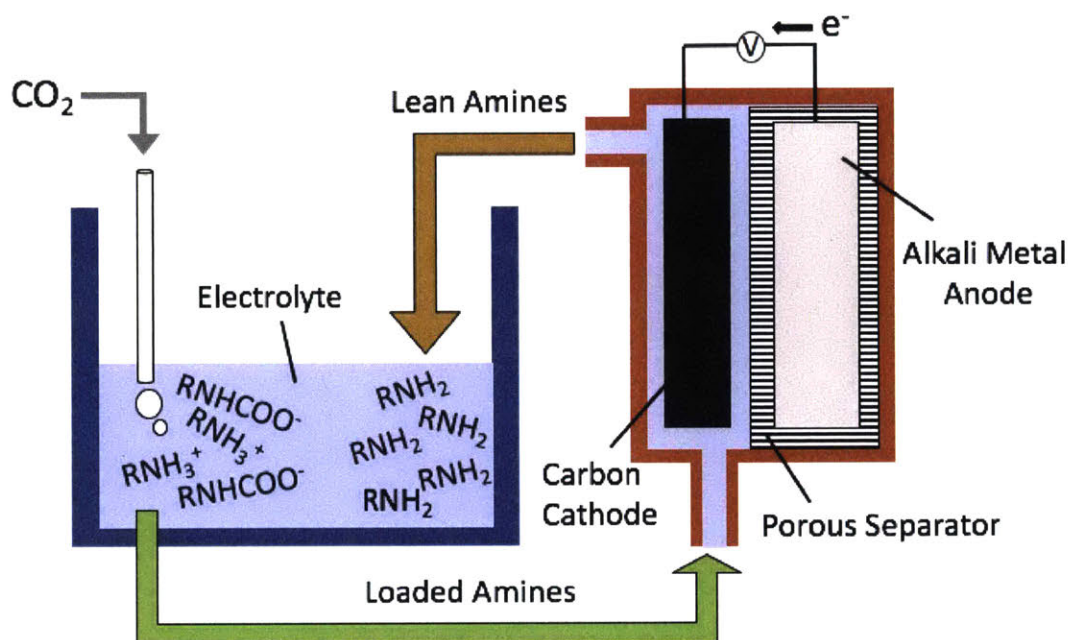


Figure 5-1: Schematic of an amine-mediated electrochemical CO₂ reduction process in non-aqueous media.

Additionally, the effect of the cation size and nature on the reduction potential of loaded amine species will also be studied in the future. Preliminary DFT calculations on this system presence of Li cations is necessary for the reduction of carbamate species. This suggests that the cation in the electrolyte plays a key role in determining the outcome of the electrochemical reduction of loaded amine species. In line with this understanding, future work will explore if and how different sized cations such as Na⁺, and TBA⁺ affect the reaction kinetics and/or reaction pathway.

Furthermore, previous studies have shown that varying the structure of the CO₂ sorbent can alter the CO₂ binding geometry i.e. the extent to which the CO₂ molecule bends upon complexation with the sorbent.³¹ Therefore, another aspect that future work will focus on is understanding how modulating the amine structure will affect the potential of electron transfer to a loaded amine specie. Amines that are able to bend the CO₂ to a larger degree are likely to

have shorter –N-C- bond lengths,³¹ which could in turn affect kinetics of the electrochemical reduction process.

Lastly, future work will also explore the possibility of translating this system to an alternate metal-gas system like Na-CO₂ or Ca-CO₂. The main motivation behind switching to calcium or sodium as the alkali metal for the anode is that they are far more abundant and cheaper than Li metal. A calcium-CO₂ system like the one proposed above would be particularly attractive because of the potential of forming calcium carbonate, which is of wide industrial and commercial use.

6 REFERENCES

- 1 EPA, A. Inventory of U.S. Greenhouse Gas Emissions and Sinks: 1990-2014. *Environmental Protection Agency 2016* (2016).
- 2 Stern, M. C., Simeon, F., Herzog, H. & Hatton, T. A. Post-combustion carbon dioxide capture using electrochemically mediated amine regeneration. *Energy & Environmental Science* **6**, 2505, doi:10.1039/c3ee41165f (2013).
- 3 United Nations Framework Convention on Climate Change. *The Paris Agreement*, <http://unfccc.int/paris_agreement/items/9485.php> (2017).
- 4 Center for Climate and Energy Solutions. *EPA Regulation of Greenhouse Gas Emissions from New Power Plants*, <<https://www.c2es.org/federal/executive/epa/ghg-standards-for-new-power-plants>> (2016).
- 5 Zevenhoven, R. & Kilpinen, P. *Control of pollutants in flue gases and fuel gases*. (Helsinki University of Technology Espoo, Finland, 2001).
- 6 GHG, I. CO₂ capture in the cement industry. *Report 3*, 2008 (2008).
- 7 Herzog, H., Meldon, J. & Hatton, A. Advanced post-combustion CO₂ capture. *Clean Air Task Force*, 1-39 (2009).
- 8 Beér, J. M. High efficiency electric power generation: The environmental role. *Progress in Energy and Combustion Science* **33**, 107-134 (2007).
- 9 Coninck, H. d. *et al.* Carbon capture and storage in industrial applications: Technology synthesis report. *Policy Studies* **2012**, 2011 (2013).
- 10 Sullivan, B. P., Krist, K. & Guard, H. *Electrochemical and electrocatalytic reactions of carbon dioxide*. (Elsevier, 2012).
- 11 Kolomnikov, I. Reactions of carbon dioxide with transition metal compounds. *Pure and Applied Chemistry* **33**, 567-582 (1973).
- 12 Kortunov, P. V., Siskin, M., Baugh, L. S. & Calabro, D. C. In Situ Nuclear Magnetic Resonance Mechanistic Studies of Carbon Dioxide Reactions with Liquid Amines in Non-aqueous Systems: Evidence for the Formation of Carbamic Acids and Zwitterionic Species. *Energy & Fuels* **29**, 5940-5966, doi:10.1021/acs.energyfuels.5b00985 (2015).
- 13 Kortunov, P. V., Baugh, L. S., Siskin, M. & Calabro, D. C. In Situ Nuclear Magnetic Resonance Mechanistic Studies of Carbon Dioxide Reactions with Liquid Amines in Mixed Base Systems: The Interplay of Lewis and Brønsted Basicities. *Energy & Fuels* **29**, 5967-5989, doi:10.1021/acs.energyfuels.5b00988 (2015).
- 14 Stern, M. C. *Electrochemically-Mediated Amine Regeneration for Carbon Dioxide Separations*, Citeseer, (2013).
- 15 Kortunov, P. V., Siskin, M., Baugh, L. S. & Calabro, D. C. In Situ Nuclear Magnetic Resonance Mechanistic Studies of Carbon Dioxide Reactions with Liquid Amines in Aqueous Systems: New Insights on Carbon Capture Reaction Pathways. *Energy & Fuels* **29**, 5919-5939, doi:10.1021/acs.energyfuels.5b00850 (2015).
- 16 Rochelle, G. T. Amine scrubbing for CO₂ capture. *Science* **325**, 1652-1654, doi:10.1126/science.1176731 (2009).
- 17 Global CCS Institute. *The Global Status of CCS: 2016, Summary Report*, Australia. (2016).

- 18 Boot-Handford, M. E. *et al.* Carbon capture and storage update. *Energy Environ. Sci.* **7**, 130-189, doi:10.1039/c3ee42350f (2014).
- 19 Bara, J. E., Camper, D. E., Gin, D. L. & Noble, R. D. Room-temperature ionic liquids and composite materials: platform technologies for CO₂ capture. *Accounts of Chemical Research* **43**, 152-159 (2009).
- 20 Rogers, R. D. & Seddon, K. R. Ionic liquids--solvents of the future? *Science* **302**, 792-793 (2003).
- 21 Brennecke, J. F. & Gurkan, B. E. Ionic liquids for CO₂ capture and emission reduction. *The Journal of Physical Chemistry Letters* **1**, 3459-3464 (2010).
- 22 Cadena, C. *et al.* Why is CO₂ so soluble in imidazolium-based ionic liquids? *Journal of the American Chemical Society* **126**, 5300-5308 (2004).
- 23 Anderson, J. L., Dixon, J. K. & Brennecke, J. F. Solubility of CO₂, CH₄, C₂H₆, C₂H₄, O₂, and N₂ in 1-Hexyl-3-methylpyridinium Bis (trifluoromethylsulfonyl) imide: Comparison to Other Ionic Liquids. *Accounts of chemical research* **40**, 1208-1216 (2007).
- 24 Ramdin, M., de Loos, T. W. & Vlucht, T. J. State-of-the-art of CO₂ capture with ionic liquids. *Industrial & Engineering Chemistry Research* **51**, 8149-8177 (2012).
- 25 Gurkan, B. E. *et al.* Equimolar CO₂ absorption by anion-functionalized ionic liquids. *Journal of the American Chemical Society* **132**, 2116-2117 (2010).
- 26 Wang, C. *et al.* Tuning the basicity of ionic liquids for equimolar CO₂ capture. *Angewandte Chemie International Edition* **50**, 4918-4922 (2011).
- 27 H. Davis, J., James. Task-specific ionic liquids. *Chemistry letters* **33**, 1072-1077 (2004).
- 28 Bates, E. D., Mayton, R. D., Ntai, I. & Davis, J. H. CO₂ capture by a task-specific ionic liquid. *Journal of the American Chemical Society* **124**, 926-927 (2002).
- 29 Camper, D., Bara, J. E., Gin, D. L. & Noble, R. D. Room-temperature ionic liquid-amine solutions: Tunable solvents for efficient and reversible capture of CO₂. *Industrial & Engineering Chemistry Research* **47**, 8496-8498 (2008).
- 30 Gutowski, K. E. & Maginn, E. J. Amine-functionalized task-specific ionic liquids: a mechanistic explanation for the dramatic increase in viscosity upon complexation with CO₂ from molecular simulation. *Journal of the American Chemical Society* **130**, 14690-14704 (2008).
- 31 Gurkan, B. *et al.* Molecular Design of High Capacity, Low Viscosity, Chemically Tunable Ionic Liquids for CO₂Capture. *The Journal of Physical Chemistry Letters* **1**, 3494-3499, doi:10.1021/jz101533k (2010).
- 32 Trilla, M. *et al.* Ionic liquid crystals based on mesitylene-containing bis-and trisimidazolium salts. *Langmuir* **24**, 259-265 (2008).
- 33 Whipple, D. T. & Kenis, P. J. A. Prospects of CO₂Utilization via Direct Heterogeneous Electrochemical Reduction. *The Journal of Physical Chemistry Letters* **1**, 3451-3458, doi:10.1021/jz1012627 (2010).
- 34 Oloman, C. & Li, H. Electrochemical processing of carbon dioxide. *ChemSusChem* **1**, 385-391, doi:10.1002/cssc.200800015 (2008).
- 35 Kuhl, K. P., Cave, E. R., Abram, D. N. & Jaramillo, T. F. New insights into the electrochemical reduction of carbon dioxide on metallic copper surfaces. *Energy & Environmental Science* **5**, 7050, doi:10.1039/c2ee21234j (2012).

- 36 Chandrasekaran, K. & Bockris, L. M. In-situ spectroscopic investigation of adsorbed intermediate radicals in electrochemical reactions: CO₂⁻ on platinum. *Surface science* **185**, 495-514 (1987).
- 37 Bockris, J. M. & Wass, J. On the photoelectrocatalytic reduction of carbon dioxide. *Materials chemistry and physics* **22**, 249-280 (1989).
- 38 Chaplin, R. & Wragg, A. Effects of process conditions and electrode material on reaction pathways for carbon dioxide electroreduction with particular reference to formate formation. *Journal of Applied Electrochemistry* **33**, 1107-1123 (2003).
- 39 Chen, Y., Li, C. W. & Kanan, M. W. Aqueous CO₂ reduction at very low overpotential on oxide-derived Au nanoparticles. *Journal of the American Chemical Society* **134**, 19969-19972 (2012).
- 40 Li, C. W. & Kanan, M. W. CO₂ reduction at low overpotential on Cu electrodes resulting from the reduction of thick Cu₂O films. *Journal of the American Chemical Society* **134**, 7231-7234 (2012).
- 41 Zheng, C., Tan, J., Wang, Y. J. & Luo, G. S. CO₂ Solubility in a Mixture Absorption System of 2-Amino-2-methyl-1-propanol with Glycol. *Industrial & Engineering Chemistry Research* **51**, 11236-11244, doi:10.1021/ie3007165 (2012).
- 42 Gattrell, M., Gupta, N. & Co, A. A review of the aqueous electrochemical reduction of CO₂ to hydrocarbons at copper. *Journal of Electroanalytical Chemistry* **594**, 1-19, doi:10.1016/j.jelechem.2006.05.013 (2006).
- 43 Schouten, K., Kwon, Y., Van der Ham, C., Qin, Z. & Koper, M. A new mechanism for the selectivity to C 1 and C 2 species in the electrochemical reduction of carbon dioxide on copper electrodes. *Chemical Science* **2**, 1902-1909 (2011).
- 44 Xu, S., Das, S. K. & Archer, L. A. The Li-CO₂ battery: a novel method for CO₂ capture and utilization. *RSC Advances* **3**, 6656, doi:10.1039/c3ra40394g (2013).
- 45 Gowda, S. R., Brunet, A., Wallraff, G. M. & McCloskey, B. D. Implications of CO₂ Contamination in Rechargeable Nonaqueous Li-O₂ Batteries. *J Phys Chem Lett* **4**, 276-279, doi:10.1021/jz301902h (2013).
- 46 Lim, H. K. *et al.* Toward a lithium-"air" battery: the effect of CO₂ on the chemistry of a lithium-oxygen cell. *J Am Chem Soc* **135**, 9733-9742, doi:10.1021/ja4016765 (2013).
- 47 Xu, K. Nonaqueous liquid electrolytes for lithium-based rechargeable batteries. *Chemical reviews* **104**, 4303-4418 (2004).
- 48 Takechi, K., Shiga, T. & Asaoka, T. A Li-O₂/CO₂ battery. *Chem Commun (Camb)* **47**, 3463-3465, doi:10.1039/c0cc05176d (2011).
- 49 Read, J. *et al.* Oxygen transport properties of organic electrolytes and performance of lithium/oxygen battery. *Journal of The Electrochemical Society* **150**, A1351-A1356 (2003).
- 50 Read, J. Ether-based electrolytes for the lithium/oxygen organic electrolyte battery. *Journal of The Electrochemical Society* **153**, A96-A100 (2006).
- 51 Aschenbrenner, O. & Styring, P. Comparative study of solvent properties for carbon dioxide absorption. *Energy & Environmental Science* **3**, 1106, doi:10.1039/c002915g (2010).
- 52 Aydin, G., Karakurt, I. & Aydiner, K. Evaluation of geologic storage options of CO₂: Applicability, cost, storage capacity and safety. *Energy Policy* **38**, 5072-5080, doi:10.1016/j.enpol.2010.04.035 (2010).

- 53 Yoo, E. & Zhou, H. Li– air rechargeable battery based on metal-free graphene nanosheet catalysts. *ACS nano* **5**, 3020-3026 (2011).
- 54 Bazito, F. F. C., Kawano, Y. & Torresi, R. M. Synthesis and characterization of two ionic liquids with emphasis on their chemical stability towards metallic lithium. *Electrochimica Acta* **52**, 6427-6437, doi:10.1016/j.electacta.2007.04.064 (2007).
- 55 Lu, Y.-C., Gasteiger, H. A. & Shao-Horn, Y. Method development to evaluate the oxygen reduction activity of high-surface-area catalysts for Li-air batteries. *Electrochemical and Solid-State Letters* **14**, A70-A74 (2011).
- 56 Lu, Y.-C., He, Q. & Gasteiger, H. A. Probing the Lithium–Sulfur Redox Reactions: A Rotating-Ring Disk Electrode Study. *The Journal of Physical Chemistry C* **118**, 5733-5741 (2014).
- 57 Lu, Y.-C. *et al.* Lithium–oxygen batteries: bridging mechanistic understanding and battery performance. *Energy & Environmental Science* **6**, 750-768 (2013).
- 58 Girishkumar, G., McCloskey, B., Luntz, A., Swanson, S. & Wilcke, W. Lithium– air battery: promise and challenges. *The Journal of Physical Chemistry Letters* **1**, 2193-2203 (2010).
- 59 Gallant, B. M. *et al.* Chemical and morphological changes of Li–O₂ battery electrodes upon cycling. *The Journal of Physical Chemistry C* **116**, 20800-20805 (2012).
- 60 Zhang, X. *et al.* Rechargeable Li-CO₂ batteries with carbon nanotubes as air cathodes. *Chem Commun (Camb)* **51**, 14636-14639, doi:10.1039/c5cc05767a (2015).
- 61 Zhang, Z. *et al.* The First Introduction of Graphene to Rechargeable Li-CO₂ Batteries. *Angew Chem Int Ed Engl* **54**, 6550-6553, doi:10.1002/anie.201501214 (2015).
- 62 Addadi, L., Raz, S. & Weiner, S. Taking Advantage of Disorder: Amorphous Calcium Carbonate and Its Roles in Biomineralization. *Advanced Materials* **15**, 959-970, doi:10.1002/adma.200300381 (2003).
- 63 Foran, E., Weiner, S. & Fine, M. Biogenic fish-gut calcium carbonate is a stable amorphous phase in the gilt-head seabream, *Sparus aurata*. *Scientific reports* **3** (2013).
- 64 Yin, W., Grimaud, A., Lepoivre, F., Yang, C. & Tarascon, J. M. Chemical vs Electrochemical Formation of Li₂CO₃ as a Discharge Product in Li–O₂/CO₂ Batteries by Controlling the Superoxide Intermediate. *The journal of physical chemistry letters* **8**, 214-222 (2016).
- 65 Thompson, A. Electrochemical potential spectroscopy: a new electrochemical measurement. *Journal of The Electrochemical Society* **126**, 608-616 (1979).
- 66 Barzagli, F., Lai, S. & Mani, F. Novel non-aqueous amine solvents for reversible CO₂ capture. *Energy Procedia* **63**, 1795-1804, doi:10.1016/j.egypro.2014.11.186 (2014).
- 67 Brennecke, J. F. & Gurkan, B. E. Ionic Liquids for CO₂Capture and Emission Reduction. *The Journal of Physical Chemistry Letters* **1**, 3459-3464, doi:10.1021/jz1014828 (2010).